Rijksuniversiteit Groningen

Bachelor Thesis

Effect of Broken Channels on the Performance of the NeuLAND Neutron Detector

Author:
S. H. Bijl
S3124746

Supervisor
N. Kalantar-Nayestanaki
Second Examiner
J.G. Messchendorp

July 7, 2020

Abstract

NeuLAND has been designed to perform a full kinematic reconstruction of the four momentum of a detected neutron. This research focuses on the effect of broken channels on the full neutron reconstruction. During an experiment with beams, it can happen that a channel breaks down and remains off throughout the whole experiment. This can have consequences on the full neutron reconstruction. This effect is studied with the use of simulated data with twelve double planes with neutron energies of 200, 600 and 1000 MeV. The analysis was done with the use of the Deep Neural Network (DNN) and by extracting the efficiency and constructing the invariant mass (inv. mass) spectrum. The DNN method is a relatively new method, therefor, an already existing caliometric method was used as a verification. As a first approximation a study was performed by turning off a percentage of channels, which were chosen randomly for each simulated event (Stochastic Shut-Off Scenario). The percentage of broken channels was varied in the range of $0 - 20\%$ with increments of 5%. The DNN showed a decrease in efficiency for all number neutron multiplicities and percentages of broken channels for 200 and 600 MeV. At 1000 MeV an increase was seen for events with neutron multiplicities of one to four. A second study was done were the most crucial modules, eight scintillator bars stacked next to each other, were turned off throughout the simulation with a neutron energy of 600 MeV. For this scenario the conclusion was made that the number of counts in the reconstructed peak shows a decrease of 1.0% for the DNN with one broken module for neutron multiplicity-two events. With two and three broken modules there is an increase of 1.5% and 2.1% respectively. In addition to this loss/gain in efficiency there was also an internal shift in the inv. mass observed. This is due to the effect of the DNN which will favour clusters that lie closer to the beam with increasing number of broken channels.

Contents

1 Introduction **1**
- 1.1 FAIR . . . 1
  - 1.1.1 NUSTAR . . . 1
  - 1.1.2 R3B . . . 2
  - 1.1.3 NeuLAND . . . 3
- 1.2 Broken Channels . . . 3

2 Neutron-Track Reconstruction **5**
- 2.1 Overview of the Method . . . 5
- 2.2 Clustering and Neutron Selection . . . 6
- 2.3 TDR Method . . . 6
- 2.4 Scoring Method . . . 8
- 2.5 Deep Neural Network (DNN) Method . . . 8
  - 2.5.1 Multiplicity Determination . . . 9
  - 2.5.2 Hit Selection . . . 9
  - 2.5.3 DNN Training . . . 9
- 2.6 Model Dependence . . . 10

3 Broken Channels **11**
- 3.1 Stochastic Shut-Off Scenario . . . 12
  - 3.1.1 Multiplicity Efficiency . . . 12
  - 3.1.2 Hit Selection . . . 16
- 3.2 Worst-Case Scenario . . . 20
  - 3.2.1 Most Crucial Channels . . . 20
  - 3.2.2 Broken Modules Scenario . . . 21
  - 3.2.3 Comparison between the Stochastic and Worst-Case Scenarios . . . 24

4 Discussion **26**

5 Conclusions **28**

6 Appendix **32**

1 Introduction

This section will describe the role that NeuLAND (New Large Area Neutron Detector) holds within the R3B research collaboration of NUSTAR – the new facility that is being built in Darmstadt and the effect of broken channels on the performance of NeuLAND.

1.1 FAIR

GSI Helmholtz Centre for Heavy Ion Research is an existing facility with remarkable experiments such as the discovery of six new elements. The new Facility for Antiproton and ion Research (FAIR) will be an upgrade to expand the research capabilities for the international research community in various fields. [1]. An overview of the existing and planned facilities can be seen in Fig. 1.

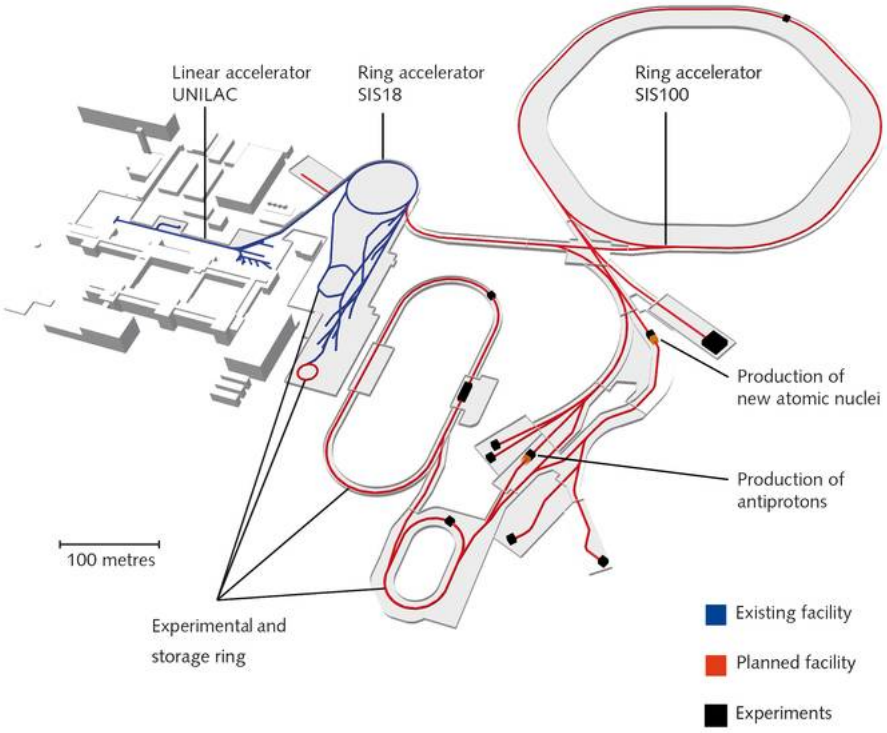

Figure 1: An illustration of the currently existing (GSI) and upcoming facility (FAIR) [8].

With the headline "The universe in the laboratory" [1], the new facility will hold four experimental collaborators: NUSTAR, CBM, PANDA and APPA. The main new feature of FAIR is the SIS100 accelerator which will be able to accelerate the particles up to 99% of the speed of light while increasing the intensity by a factor of 10,000 compared to the SIS18 ring accelerator [1].

1.1.1 NUSTAR

NUSTAR stand for the NUclear STructure, Astrophysics and Reactions. The main question that the collaboration tries to answer is how heavy elements are created in stars and stellar explosions and what the structure properties of unstable nuclei are [2]. The main piece of

experimental equipment used by NUSTAR is the new Super-FRagment Separator (Super-FRS, Fig.2). In the Super-FRS, heavy elements that leave the SIS100 with relativistic speeds are shot at a fixed target which creates a cocktail of particles including rare isotopes. The Super-FRS is an in-flight separator that can filter out any desired nucleus from the fragments produced at the Production Target within an energy range of 100 MeV - 1.5 GeV. Due to the way in which the Super-FRS is operable it enables the study of rare radioactive isotopes with short half-life times [3]. The features that the new Super-FRS will provide makes FAIR unique in the field of nuclear physics. The entire facility is planned to be ready for first operation in 2025.

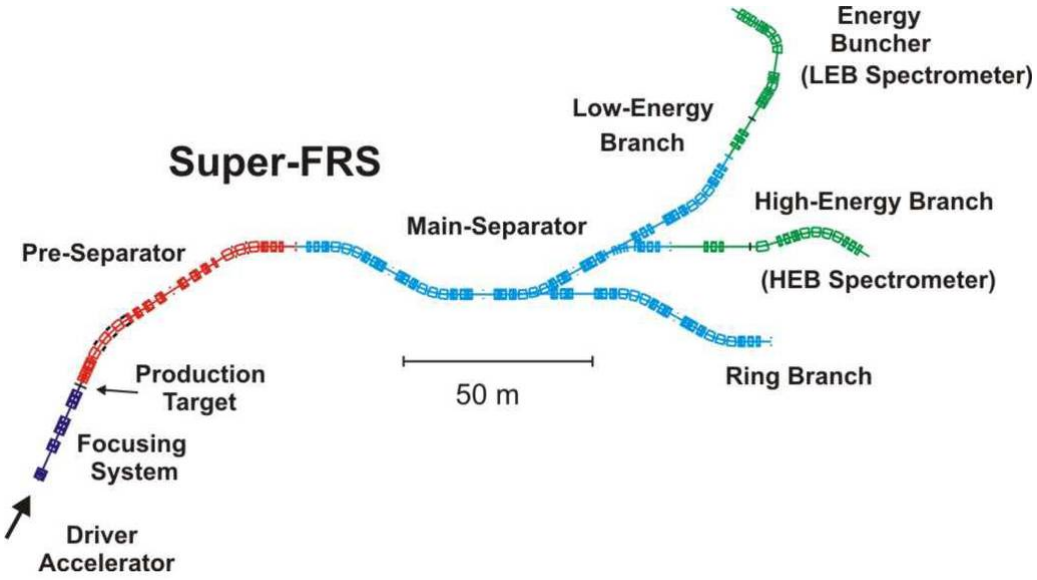

Figure 2: Layout of the Superconducting Fragment Separator [3].

When leaving the Super-FRS the particles can travel to three stations: The Low Energy Branch, the High Energy Branch, and the Ring Branch; see Fig. 2. The R3B experimental setup is located at the end of the high-energy branch of the Super-FRS.

1.1.2 R3B

R3B is a collaboration which aims to do a full kinematic reconstruction of Reactions with Relativistic Radioactive Beams (R3B) [4]. The research is focused on exotic nuclei that are created in the Super-FRS. However, these particles can be extremely rare. The nuclei of exotic isotopes are guided by the Super-FRS towards R3B where the radioactive beam hits a fixed target which induces another nuclear reaction. The CALIFA (CALorimeter for In-Flight detection of gamma-rays and high energy charged pArticles) encapsulates the target in order to achieve a total absorption of gamma-rays and protons [6]. The beam induced by the collision with the target consists of charged particles, photons, and neutrons. At the centre of R3B, downstream of CALIFA, stands the GSI Large Acceptance Dipole Magnet (GLAD) [7]. GLAD cuts the stream of reaction products into 3 distinct particle streams: protons, nuclei and neutrons, which are all guided to their respective set of detectors [7]. Due to their lack of charge, the neutrons will fly straight towards NeuLAND. An overview of the R3B setup can be found in Fig. 3.

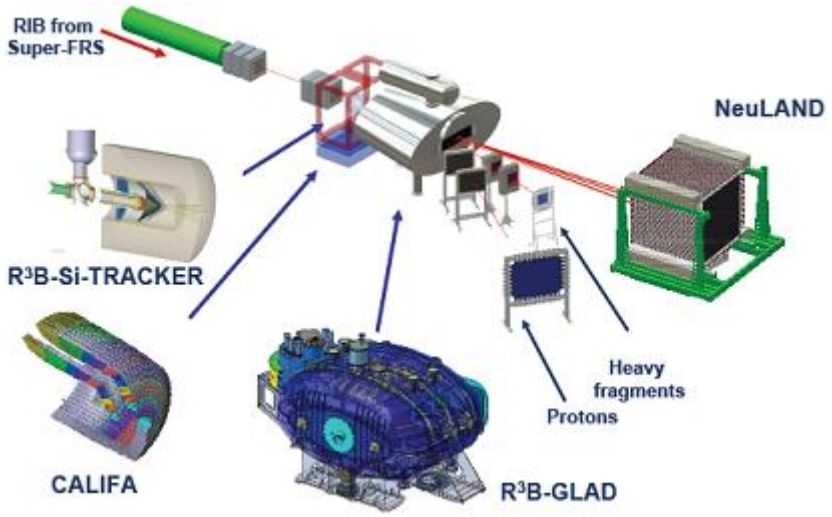

Figure 3: A schematic overview of the R3B setup at GSI/FAIR [4].

1.1.3 NeuLAND

NeuLAND is the new neutron detector for R3B, which is still under development. NeuLAND aims to reconstruct the neutrons' 4-momenta from their time-of-flight and distance between the reaction at the R3B target and their first collision with NeuLAND. The energy range in which it will operate is between 200 and 1000 MeV [9]. The distance between the target and NeuLAND is 14 m [13]. The detector consists of a row of *double planes*, which are stacked behind each other. One double plane consist of two planes of fifty scintillator bars each, one horizontally and one vertically oriented. Therefore, one double plane consists of a hundred scintillator bars. The dimensions of one double plane are 10 cm $\times$ 250 cm $\times$ 250 cm and a single scintillator has dimensions is 5 cm $\times$ 5 cm $\times$ 250 cm. Each scintillator bar is equipped with two Photon-Multiplier Tubes (PMTs), one on each end. The PMTs of eight scintillator bars are connected to a single electronic module which receive and transmit the signals. Based on the required momentum resolutions for some high-precision measurements, the most ideal time and position resolutions of NeuLAND are $\sigma_t < 150$ ps and $\sigma_{x,y,z} \approx 1.5$ cm [12]. From simple geometrical dimensions and a time resolution of around 100 ps, a spacial resolution of about 5 cm is obtained in all directions (in the direction of the light propagation along the scintillator, this is somewhat more). The current version of the NeuLAND detector at GSI can be seen in Fig. 4.

At the moment of the present study (2020), there are eight fully functioning double planes. An extra four will be installed in the near future. Eventually, the completed setup of NeuLAND will consist of thirty double planes, which are needed for the accuracy that is required for the precision of full neutron kinematic reconstruction [9]. The next step for NeuLAND will be sixteen double planes for which the funding is being sought.

1.2 Broken Channels

In this bachelor thesis the effects of broken channels on the performance of NeuLAND will be studied with simulated data. During beam time, it can happen that the hardware that receives and transmits signals from the PMTs break down. The PMTs of eight scintillator bars stacked right next to each other are connected to one electronic module. During an experiment it can

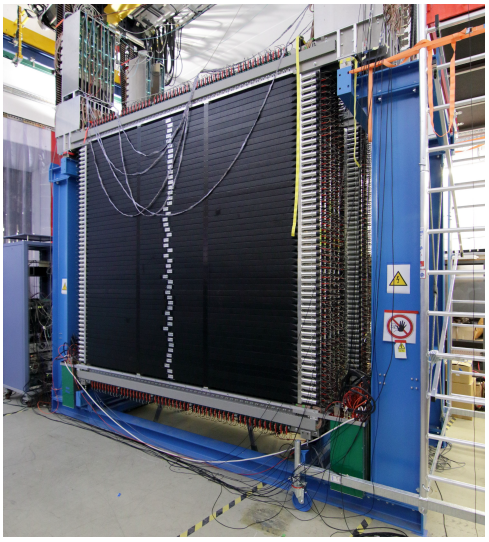

Figure 4: Front view of the NeuLAND detector at GSI [18].

happen that such a module breaks down [10]. A single scintillator bar, including its hardware, which does not give any signals will be referred to as a *broken channel*. The effect of broken channels can have a consequence on the prediction that is made on the number of neutrons in an event, which cannot be known a priori. Likewise, it can cause the signal that is being used for the full neutron reconstruction to be last, altering the reconstructed neutron four-momentum vector. The effect of broken channels on the NeuLAND performance has not yet been studied. The study was carried out using the simulation software from C. A. Douma [14, 23]. The analysis methods used are the conventional caliometric Technical Design Report (TDR) method [12] and a new method based on artificial intelligence: the Deep Neural Network (DNN) method [13]. The study was done by looking at the efficiency loss/gain and the invariant mass spectra of the DNN method in the case of broken channels [13]. The efficiency is the percentage of right predictions of the number of neutrons that were in an event. The DNN method is a fairly new method and has not yet been tested during an experiment. Therefore, the results were compared to the already existing and proven-effective TDR method [11, 12]. The upcoming experiments with NeuLAND will be with twelve double planes, therefore the simulations for this thesis were done with twelve double planes. Two scenarios will be analysed: a Stochastic Shut-Off Scenario where with each event random channels will be turned off (further explanation in Sect. 3.1) and a Worst-Case Scenario where the most crucial modules will be turned off for each event. A module is a group of electronics which receives the signals of eight scintillator bars stacked right next to each other. In order to be able to study the Worst-Case Scenario, additional research has been performed to find the most crucial channels. This research was done by looking at the effect of turning off the most crucial channels for three different categories on the inv. mass spectrum. The three categories were: the channel which contained the most signals, the highest number of first neutron hits, and the the most energy deposit. 2.5.2).

2 Neutron-Track Reconstruction

Within R3B the aim is to do a full kinematic reconstruction of the reaction of interest [4]. NeuLAND is designed to measure the momentum four-vector of the neutrons. However, neutron reconstruction is a complicated procedure. In this chapter it will be explained why this procedure is non-trivial and which solutions exist today.

During an experiment neutrons travel towards NeuLAND, where they may collide with the detector. By means of hadronic scattering the neutron can induce a particle shower. These secondary particles consist of charged particles and photons. It are these secondary particles that can produce a signal. From each of these signals the energy deposit, time, and, position are constructed $\{E, t, x, y, z\}$ [13]. The energy deposit (E) and time (t) are obtained from the PMT signals. The longitudinal coordinate (x or y axis), dependent on the scintillator bar being oriented vertical or horizontal, can also be reconstructed from the PMT signals. From the geometry of the detector the remaining position coordinates can be constructed.

In the case where one does a neutron reconstruction with a one-neutron event, a kinematic neutron reconstruction is easily accomplished. The signal whose time variable has the shortest time-of-flight will be assigned the first hit − the first neutron collision. However, this task can get more challenging in the case of a multi-neutron event. The first neutron will still be labelled by the previously mentioned procedure but the other neutron collisions have to be picked out of an abundance of detector signals. It can even happen that neutron showers overlap and at higher energies the amount of particles created will grow rapidly making this challenge even more daunting. During an experiment, one cannot know the number of neutrons that were in the event and whether these neutrons have collided with the detector or have passed through. Therefore, in order to do a full neutron reconstruction one first needs to find out how many neutrons were in the event (neutron multiplicity) and which signals came from the first neutron collisions [14].

Neutron multiplicity can never be known with absolute certainty during an experiment, because there is no way to verify the prediction made about the number of neutrons that were in the event. When the Multiplicity Prediction is performed, the next step will be to predict which signal stems from the first interaction of a neutron with the detector − the first hit. The signals that are predicted to be a first hit will be referred to as a *showerhead*. From the *showerheads* of an event a reconstruction of the 4-momenta of the neutrons can be done based on the time-of-flight and the distance travelled of all the neutrons. Thus, the full neutron reconstruction is based on two steps: Multiplicity Prediction and Hit Selection.

2.1 Overview of the Method

In Fig. 5 an overview is given on how the NeuLAND data analysis is done. The hits contain five observables: $\{E, t, x, y, z\}$. These data can come from experiments or from simulation. Clustering which is the process of grouping signals will be explained in Sect. 2.2. One DNN is used for each of the final two steps: Multiplicity Determination and Hit Selection [13].

For the Monte Carlo simulations, Geant4 was used [16]. The framework that was used to perform the simulations was R3BRoot [17] - a software framework which is developed for simulations and data analysis for the R3B collaboration. The dimensions of the detector that were used in the simulation was the same as those used in Ref. [14] in the case of twelve double planes. The physics list used for this experiment is QGSP_INCLXX_HP. A physics list

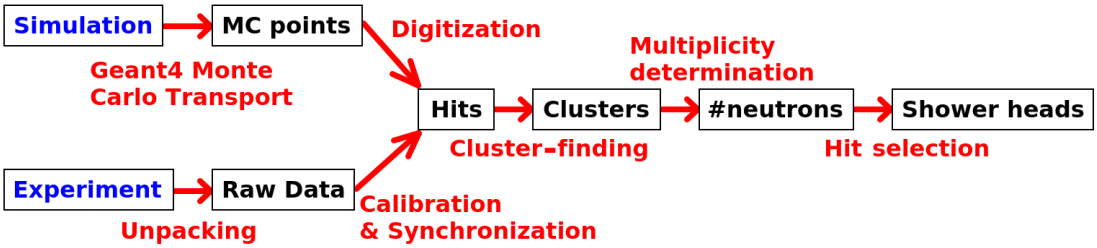

Figure 5: An overview of the steps required for the NeuLAND data analysis. The top branch illustrates simulated data and the bottom branch experimental data [13].

comparison was done in Ref. [11]. The study was done by benchmarking experimental data to the physics lists. It was found that experimental data was roughly half way between the results that were obtained by using QGSP_INCLXX_HP and QGSP_BERT_HP. R3BRoot uses QGSP_INCLXX_HP as its default physics list [11]. The event generator comes from simulation used for the ^{132}Sn breakup reaction simulation performed by Jan Mayer with 500 KeV [11]. Many different Neural Networks are possible [15], some of these Neural Networks have been tested and compared [18]. The Multiplicity Efficiency was in the same range, but in terms of performance the Deep Neural Network (DNN) required the least amount of CPU time [18, 19] which is why it has been chosen for the present study [20].

2.2 Clustering and Neutron Selection

The neutron showers can get complicated, making it hard to choose the correct first hit. To make this easier the first step is trying to group signals that stem from the same neutron event. Grouping the signals is called *clustering*. Clustering is done with the *handshake-chain clustering* method [11]. For signals that are assumed to stem from the same event, the following condition is imposed:

$$\Delta x < 7.5 \text{ cm};\ \Delta y < 7.5 \text{ cm};\ \Delta z < 7.5 \text{ cm} \tag{1}$$

$$\Delta t \leq 1 \text{ ns} \tag{2}$$

The spatial separation ensures that signals coming from neighbouring scintillator bars can be clustered. Based on the prediction made for the multiplicity of the event, the number of first hits can be selected. This is done by predicting which clusters stem from the first interaction of the neutron with the detector. Clusters stemming from the first interaction of the neutron with the detector will be referred to as a *primary cluster* and clusters stemming from a secondary particle a *secondary cluster*, respectively. Within a single primary cluster, the hit with the shortest time-of-flight is selected as first hit.

2.3 TDR Method

The Technical Design Report (TDR) offers a simple algorithm in order to do full neutron reconstruction [12]. The TDR method is a calorimetric approach where the multiplicity is determined by the number of clusters and the total energy deposition. The Hit Selection is based upon cluster velocity and deposited energy. With the TDR method the multiplicity is determined first and then the clusters are assigned to be a primary or secondary cluster.

Clustering is done based on the procedure discussed in the previous sub-section. A correlation is made between the total number of clusters and the total amount of energy deposited in

all scintillators which are plotted in a 2D-histogram (Fig. 6).

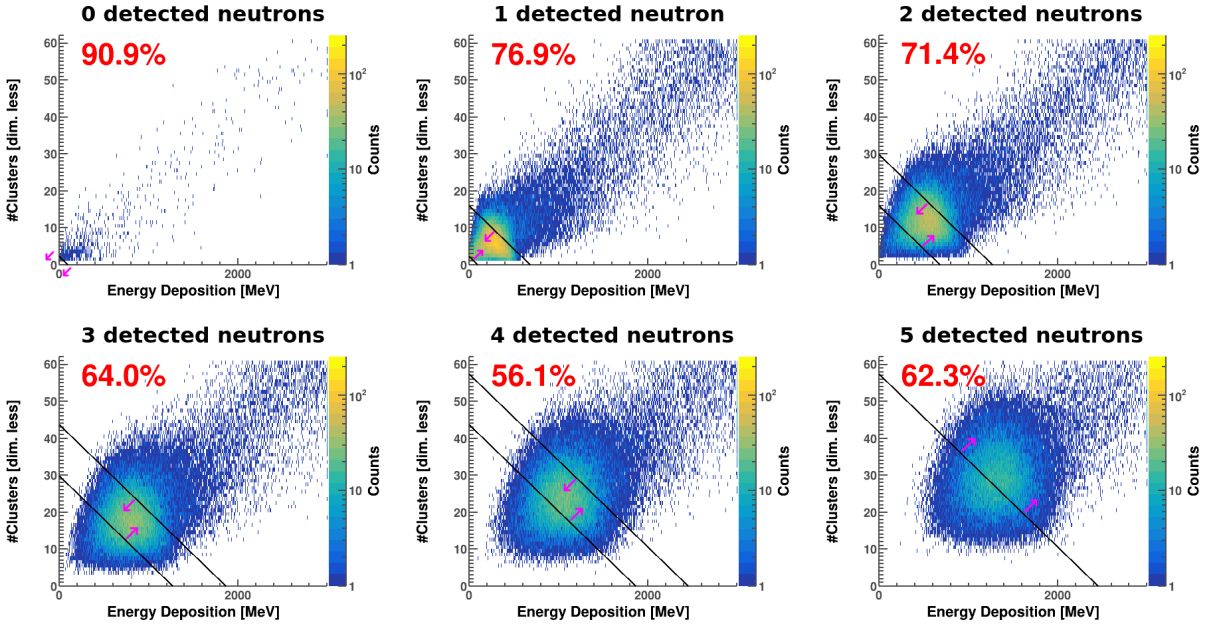

Figure 6: Illustration of the TDR method Multiplicity Determination for NeuLAND with thirty double planes and 600 MeV [14].

In Fig. 6, the 'detected neutrons' means the number of neutrons that have collided with the detector and have produced signals. From simulation number of correct Multiplicity Predictions are known and are given as a percentage in red in the top left. As can be seen in Fig. 6 the number of clusters and the total deposited energy clearly depends on the number of neutrons that were in the event.

The multiplicity is determined by making diagonal cuts in the histogram. The slope of each cut is equal for all neutron multiplicities. However, the distance between each two successive cuts can vary. The cuts are made based on the procedure used in Ref. [27]. It ensures that the largest number of events will be assigned the correct multiplicity. Keep in mind that the cuts have to be determined from simulation before an experiment. During an experiment the multiplicity is determined by finding where the count is located in the histogram [11].

When the multiplicity is determined, the clusters have to be assigned to be a primary or a secondary cluster. The first assigned primary cluster is the cluster with the shortest time-of-flight. The remaining clusters will be sorted by their respective *R-value* which is defined by:

$$R_{cluster} = \frac{|\beta_{cluster} - \beta_{beam}|}{E_{dep}^{cluster}} \tag{3}$$

where $E_{dep}^{cluster}$ is the total energy deposition in the cluster, β_{beam} is the velocity of the beam divided by the speed of light, and $\beta_{cluster}$ is given by the cluster velocity divided by the speed of light. The cluster velocity is obtained from the time-of-flight between the target and the first hit within the cluster. The Multiplicity Prediction determines the number of primary clusters. The primary clusters are those which have the lowers *R-value*. Within each primary cluster the *showerhead* is determined to be the signal with the shortest time-of-flight [11].

2.4 Scoring Method

There is a difference between primary and secondary clusters [11]. Based on their property difference, a second method has been developed called the *scoring method*. With this method all cluster data are re-valuated based on, for example, energy deposit or time-of-flight. Each quantity has a score assigned to it, e.g. a high amount of signals in the clusters gives a higher score. In order for a cluster to be assigned as primary cluster, the combined score of all cluster properties has to be higher than a set thresh-hold [11]. This method, however, only showed success in some scenarios [11]. Only after combining the scoring method with a DNN did it show its applicability and potential [14] (See Sect. 2.5.2).

2.5 Deep Neural Network (DNN) Method

Both the TDR and Scoring methods are based on pattern recognition. One helpful tool that has gotten more and more consideration in the last couple of decades is the use of Machine Learning (ML) to do data analysis and pattern recognition [15]. Since a couple of years these methods have been employed to do the data analysis for NeuLAND. This work continues on the developments made by J. Mayer and C. Douma [11, 13]. In this work, the latest attempt of these ML algorithms for NeuLAND based on the use of Deep Neural Networks (DNN) was used to study the effects of broken channels (the full algorithm is available on public domain [23]).

ML is based on the concept of the brain. Data analysis is done in three distinct steps: input signals, signal processing, and output signals, as can be seen in Fig. 7. When the sensors receive signals, e.g. sounds or visual impulses, the input travels through our brain where it gets processed and sent to our consciousness, e.g. a car is heard/ a car is seen. They key concept is the way in which data are processed: in both our brain and ML the processing happens inside a *black box*. This black box is a consequence of how ML is structured. By training the DNN it is thought to make predictions. The amount of neuron connections can vary with each DNN, even when trained for the same task. Consequently, with the black box one does not know why it does what it does, similar to our limited knowledge of how a brain processes data [15].

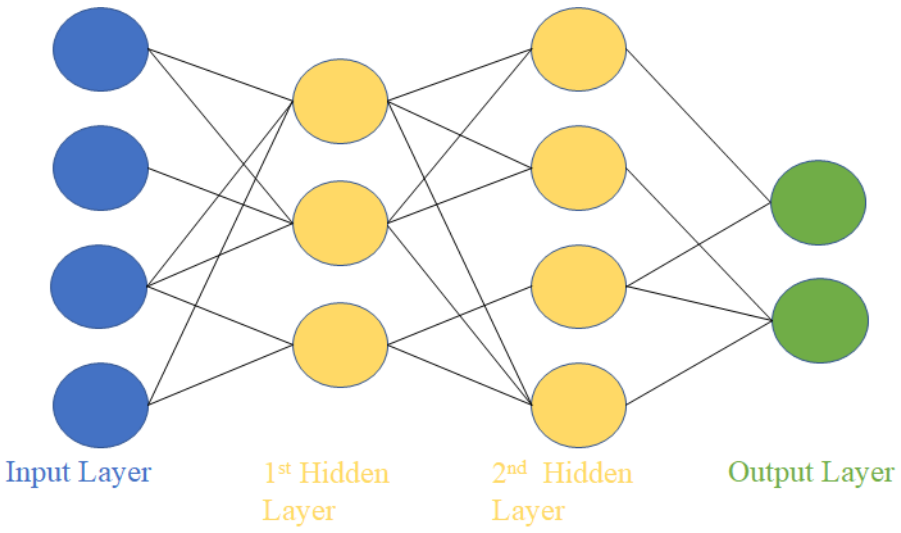

Figure 7: Schematic of a Neural Network.

In Fig. 7 an overview is shown of how an arbitrary neural network looks. The amount of neurons in each layer and the number of hidden layers can vary depending on the task of the DNN. The DNN assigns a weight to each neuron in the input layer or hidden layer which causes signals to be enhanced or impaired. All neuron connections have a weight assigned to it. The weights are assigned by using a nonlinear activation function (ReLu Function) [19]. By training the DNN the weights of a Neural Network are picked such that the DNN predicts the desired outcome. For this network the Keras [21] user-interface was used in addition to the TensorFlow [22] framework.

2.5.1 Multiplicity Determination

The first DNN is used to determine the multiplicity of an event. The input layer of the first DNN consists of a total of $4 + 400n$ neurons, where n is the total number of double planes. The input neurons include the total number of clusters, total deposited energy, and one neuron for each observable: depending on the orientation of the scintillator either the x or the y axis corresponds to the longitudinal axis. The remaining spacial position is obtained from the geometry position of the scintillator bar. In addition to the energy deposit E and the time of the signal detector t this gives a four variables for each channel. There are two hidden layers of which the first has 9000 neurons and the second 1200. In the output layer there are a total of five neurons, one for each possible multiplicity. For the output neurons a Softmax activation function is used [11, 18]. Because of this function each output neuron corresponds to a percentage − a likelihood that this is the correct multiplicity. The neuron with the largest output is assumed to correspond to the event multiplicity [18].

2.5.2 Hit Selection

A separate DNN is used for the Hit Selection. The previous step tells us the prediction of the DNN on how many neutrons were in the event and thus how many primary clusters should be looked for [14]. The second DNN works with the same principles as the scoring method (sect. 2.2). The input layer uses multiple cluster properties such as the total energy deposit in the cluster and time-of-flight. In total it has fourteen input neurons − one for each cluster property considered. The output layer consists of two neurons with a SoftMax activation function which gives a probability of the cluster being a primary cluster and a secondary cluster, similar to a score. The DNN consists of a total of twelve hidden layers with two hundred neutrons each. During a simulation all clusters go through the DNN one-by-one and each will be assigned a score based on the DNN outcome. Based on the Multiplicity Prediction of the previous step, the clusters with highest scores will be categorized as primary cluster. Within the primary cluster it is the signal with the shortest time-of-flight that is determined to be the *showerhead* [14].

2.5.3 DNN Training

The training was done with Supervise Learning (SL) [24]. Supervised Learning was used with both the AGRAD [25] minimization algorithm and the Categorical Cross Entropy [26] minimization function. In order to train the DNN events had to be generated, however, not all simulated events are usable and had to be discarded. The first criterion is that events cannot be empty because there is nothing to train with empty events. Secondly, the number of neutrons that were shot at the detector cannot be used as falsifiability criteria because it can happen that neutrons do not produce a signal in the detector. Therefore, the criteria state that only events where all neutrons produced a signal can be used for training [18]. The weights of the remaining events have to be adapted for the loss function in order to prevent a bias from the

DNN. The remaining events were separated per 1000 events. After each batch of 1000 events, two epochs wer used for training [14].

2.6 Model Dependence

It is not possible to use experimental data to do the DNN training because it cannot be known if the multiplicity is correct and if the correct *showerheads* are used. The same applies for the TDR method where the cuts are made based on simulated data. Thus, for both methods one is dependent on the model that is used for simulation [11]. The models used have three main components: the geometry, the event generator and the physics list containing information about physics processes. These models carry uncertainties with them as they do not truly mimic the conditions of an experiment. As of today the physics list still poses a major challenge for the data analysis for NeuLAND [13, 11]. Therefore, the most relevant uncertainty lies within the physics list. The physics list uncertainties have been quantified in Ref. [14] for several scenarios. The physics list uncertainty cannot be suppressed and therefor has to be taken into account in this study. The geometry of the simulation is modelled close to reality and is based on the twelve double plane simulation used in Ref. [14]. Similarly, the event generator can be modelled with sufficient realism to suppress the uncertainties.

3 Broken Channels

In the case of a broken channel the scintillator will be unable to transmit a signal. Therefore, the hit data $\{E, t, z, y, z\}$ of that scintillator bar is lost. As a result, both the total number of counts and the total energy deposited will decrease. On a smaller scale the number of counts within a cluster and the energy deposited in the cluster decrease as well. It can even occur that entire clusters are lost or that a single cluster will be broken into two or more. Another possibility is that the signal with the shortest time-of-flight within a primary cluster is lost. In the case that the cluster will still be categorized as a primary cluster the second signal with the shortest time-of-flight will be labelled as *showerhead*. Consequently, this will have an effect on the reconstructed four-momentum vector of the neutron as it is based on the wrong *showerhead* [14].

In this thesis the results will be analysed on two levels: Multiplicity Efficiency and Hit Selection. Multiplicity Efficiency is the percentage of right predictions made by the DNN or TDR method. For the Multiplicity Efficiency the effect of broken channels will be studied based on the percentage of right predictions made by the DNN and the TDR method. For the Hit Selection it is useful to look at the invariant mass spectra of the neutron events. One such possibility that might happen in the case of broken channels is that the *showerhead* signal gets lost. As mentioned above this has an effect when reconstructing the four-momentum vector of the neutrons. When the *showerhead* signal is lost and the correct multiplicity is still given to the event the effect cannot be seen in the efficiency but will be visible in the invariant mass spectrum.

For this experiment all simulations have been done with twelve double planes. The full NeuLAND detector will consist of thirty double planes at which the neutron collision probability was deemed sufficient ($> 95\%$) [12]. Upcoming experiments will be done with twelve double planes, therefore this number was chosen for this thesis. In the case of twelve double planes, with simulation and 1000 MeV neutrons, the chance of one-neutron producing signals in the detector is $\approx 80\%$ (see Fig. 10, perfect tracking for a one-neutron event with no broken channels). Consequently, the chance of all five neutrons producing signals with the detector is only $\approx 33\%$. Nevertheless, it can happen that the DNN and the TDR method give a correct Multiplicity Prediction for the event, even when not all neutrons collided with the detector. This is what will be referred to as a *false-positive* event. This effect can best be understood by looking at Fig. 6. In Fig. 6, it can be seen that some events are classified outside the correct multiplicity cuts. In the case of a four neutron event it can happen that one-neutron does not produce a signal and that the event still gets a 'correct' Multiplicity Prediction − a false-positive. This is due to the incorrect multiplicity predictions that are made for events with a neutron multiplicity of three. In order to study this effect, an additional tool is used in the simulation: *restricted multiplicity*. Restricted multiplicity is the efficiency of all correct Multiplicity Predictions without the false-positives.

Another tool that is used for the simulation is *perfect tracking*: Perfect tracking is the highest possible efficiency that can be achieved. It acts as a benchmark to see how much efficiency gain can still be achieved for both the DNN and TDR method. In the case of perfect tracking, the *showerhead* is assigned by the signal with the shortest time-of-flight between all signals that stem from the same neutron event. In the case of broken channels, perfect tracking will only lose efficiency if all signals that stem from the same neutron are lost. Keep in mind that these tools are only applicable in simulated events. During experiments the amount of false-positives cannot be measured, because it is not known beforehand how many neutrons were in the event

and it is impossible to know which signals stem from the same neutron interaction.

The training of Deep Neural Networks is done with no broken channels. Similar for the TDR method the cuts are set when doing a simulation with no broken channels. This is done in order to be able to quantify the effect of broken channels on the full neutron reconstruction.

3.1 Stochastic Shut-Off Scenario

As a first approximation during each single event, random scintillators were turned off and, hence, made unable to generate data. This is an unrealistic scenario as it does not mimic experimental conditions. During an experiment it may happen that a channel breaks down. In that case the same channel will remain broken until it is fixed. However, it cannot be known a priori how important the channels are. Therefore, a first approximation is done in order to study an average behaviour of the DNN and TDR method and to look at the importance of the channels (see Sect. 3.2.1 for the importance of the channels). The simulation was done with twelve double planes. The percentage of broken channels used was between $0 - 20\%$ with increments of 5%, which equals to sixty detectors. Each simulation used a total of one million events. This simulation was repeated with neutrons of 200, 600 and 1000 MeV. The training and simulation was done once with no broken channels for each of the neutron energies. For each neutron energy a single simulation of a total of 10^6 events were generated. The same simulation was used for all the studies of various percentages of the broken channels, where with each event random channels were shut off.

3.1.1 Multiplicity Efficiency

In Fig. 8, the Multiplicity Efficiency can be seen for one-neutron to five-neutron events. For five neutrons the multiplicity for the DNN and TDR method has a higher efficiency than the perfect tracking with no broken channels. This is purely because of the effect of false-positives and is a known effect [14]. In those cases one or more neutrons went through the detector without producing any signal. However, the correct multiplicity is still assigned to the event. The dotted line shows the Multiplicity Efficiency when all false-positives are not included. These are the *restricted multiplicities*. These two lines are below the perfect tracking efficiency in all neutron events, for all cases of various number of broken channels. The percentage of false-positives grows with increasing neutron multiplicity. For two-neutron events the ratio of false-positives with no broken channels is $\approx 18\%$. For five neutron events this is slightly above 50%. For one-neutron events it can still be possible to have false-positives, although very unlikely. In the simulation, the neutrons travel through air after leaving the GLAD magnet towards NeuLAND which makes it possible for the neutron to hit one of the air molecules. Just like a hit with the detector, the air also creates a shower of particles. These can be detected and will give a false positive. This effect can be seen in Fig. 8 for the one-neutron event.

The perfect tracking line shows a steady decrease for all neutron multiplicities with increasing number of broken channels. This is to be expected because the perfect tracking shows the highest possible Multiplicity Efficiency. Only in the case that all signals from the same neutron are lost does perfect tracking lose efficiency. For events with higher number of neutrons the perfect tracking efficiency decreases relatively more quickly with increasing number of broken channels. With multiplicity-four events at 20% broken channels the perfect tracking efficiency drops with 12.2% and 16.3% for five neutron events, respectively.

The TDR uses two inputs to determine the multiplicity: the number of clusters and the

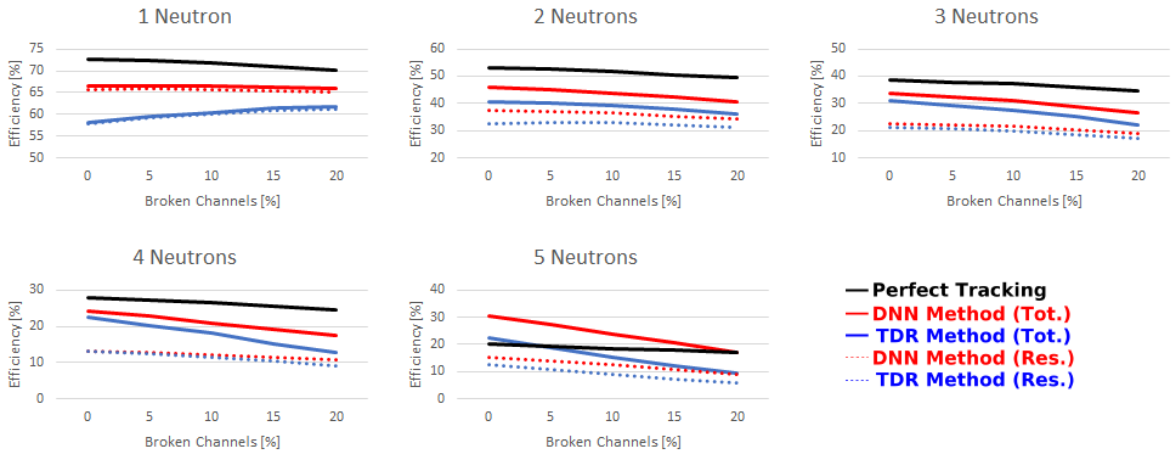

Figure 8: Detector Efficiency for various neutron multiplicities, with 200 MeV and twelve double planes.

total deposited energy, where the multiplicity is determined by the cuts that minimizes the least amount of wrong predictions (sect. [27]). In the case of broken channels, the total deposited energy can only decrease which implies that the event will move on the horizontal axis towards the left in Fig. 6. For the number of clusters there are two possibilities: clusters are lost because all signals within that cluster are lost, decreasing the total number of cluster counts in which case the event moves downwards in Fig. 6, or the cluster splits up and the total number of clusters increases and the count moves upwards along the vertical axis. From Fig. 8 one can concluded that the total energy loss and, to a lesser extent, the number of cluster losses, outweighs a possible increase in total number of clusters. This can be seen by looking at the TDR efficiency over all events with two or more neutrons. The TDR shows a decrease in efficiency for all neutron multiplicities when the percentage of broken channels increases. Only with one-neutron events does the TDR show an increase in efficiency. This increase can be explained by looking at how multiplicities are categorized with the TDR method. The TDR method can assign each event to have a multiplicity of one to five. Since the total energy deposit decreases, the chance of one-neutron events being assigned a higher multiplicity also decreases. However, a one-neutron event can only drop down to a zero-neutron event when all signals are lost. Consequently, the efficiency trade-off is positive for the one-neutron event with the TDR method, which is why we see an increase in Fig. 8 for one-neutron events. With an increasing number of neutron multiplicity, the energy that is deposited increases. Therefore, when the same percentage of detectors breaks down, the energy deposit should decrease more rapidly with a higher number of neutron multiplicity. This effect can be seen in Fig. 8: the efficiency of higher neutron multiplicities decreases more rapidly with an increasing number of neutron events. The efficiency with four neutrons goes from 22.5% with no broken channels to 12.9% with 20% broken channels, whereas with five neutron events the efficiency goes from 22.4% to 9.3%, with the TDR method.

With the DNN the same effect for one-neutron events does not seem to be present. For a multiplicity of one the DNN efficiency decreases at higher percentages of broken channels, although this is only a decrease of 0.6%. Just as with the TDR method, the DNN decides any event where there is at least one signal to have a multiplicity of at least one. But the difference between one-neutron events for both methods is that the DNN efficiency is already close to the highest achievable efficiency, therefor there is less efficiency to be gained. However, the

DNN does approach the perfect tracking efficiency with higher percentage of broken channels in the case of a one-neutron event. Therefore it can be concluded that the DNN shows a similar behaviour as the TDR for one-neutron event.

Similar to the TDR the efficiency of the DNN is more affected at higher multiplicities. The causes in both cases are the same. With increasing number of neutrons in an event, more signals will be produced. Therefore, in the case of broken channels more signals will be lost on average and thus the efficiency drops more quickly. As can be seen in Fig. 8 the biggest drop in efficiency is for the neutron multiplicity of five. In that case there is an efficiency drop of 13.5%, which is close to half of the efficiency with no broken channels. For multiplicity 2 to 4, the efficiency drop is 5.2%, 7.0%, and 7.1% respectively at 20% broken channels.

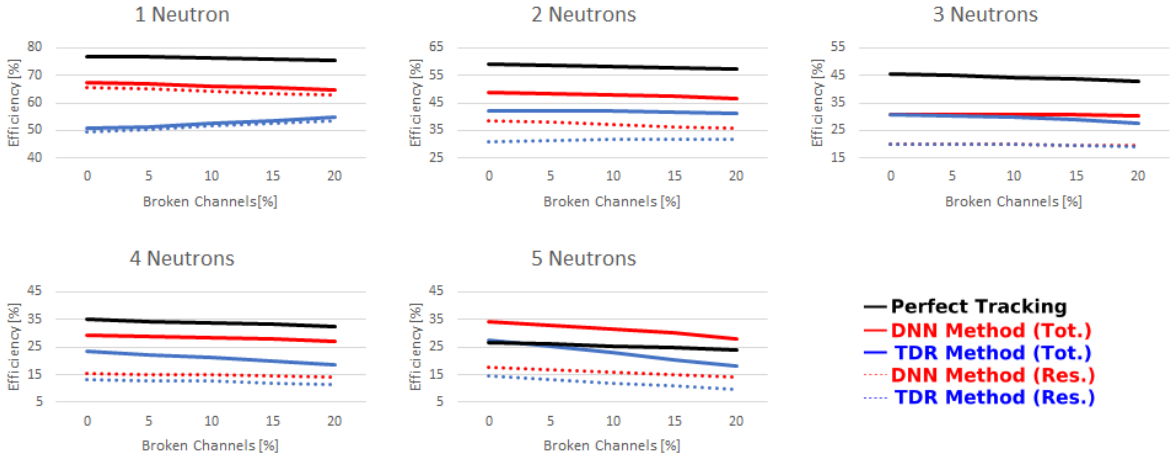

Figure 9: Same as Fig. 8 but for 600 MeV.

In Fig. 9 the NeuLAND performance is shown for 600 MeV neutrons for various multiplicities, similar to Fig. 8. The performance as a function of multiplicity for the 600 MeV neutron shows a similar behaviour as the case with 200 MeV neutrons for both the TDR and DNN method. One clear difference is that even though the trend is the same the DNN method does show a less severe efficiency loss with increasing percentage of the number of broken channels for all multiplicities.

In Fig. 10 the detector performance is shown for 1000 MeV neutrons similar to Figs. 8 and 9. At 1000 MeV the TDR does not only have an efficiency gain with one-neutron but also with multiplicity two events. Overall the effects are less severe at 1000 MeV compared to lower energies for the TDR method. At 1000 MeV the particle showers that are created are more energetic and more complex than at lower energies. This is confirmed by the perfect tracking efficiency: at higher energies the efficiency loss gets smaller with an increasing percentage of broken channels. Since the particle showers are farther reaching with many more signals, the chance of all signals being lost gets smaller. Therefor, in the case of broken channels with higher energies, the energy loss should be more severe and thus this should be reflected in the detector efficiency for various multiplicities. Additionally, the simulation is run with one million events which further decreases the chance of fluctuations and gives an overall average of the total energy lost in the case of broken channels. However, in the case of 20% broken channels, the efficiency loss is still relatively small for the TDR method, in the case of events with multiplicities 2 to 5. From this can be concluded that the number of clusters must increase due to a splitting in

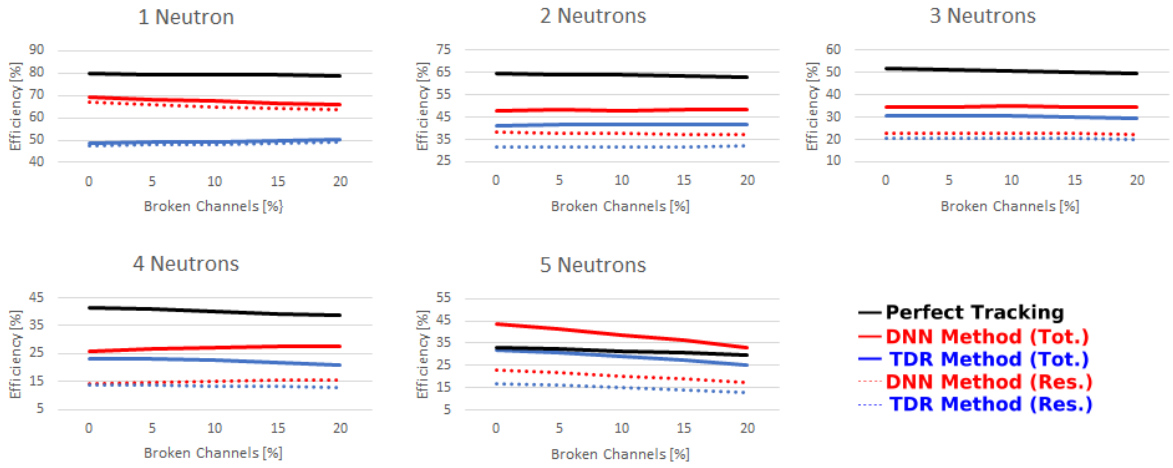

Figure 10: Same as Fig. 8 but for 1000 MeV.

clusters or that cluster count drops more slowly with higher neutron energies.

The 1000 MeV DNN detector performance shows some counter-intuitive results. In the case of events with multiplicities two to four, the DNN performance gets better with higher efficiencies with more broken channels. For events with multiplicity two and three the efficiency for the restricted DNN decreases, implying that the number of false-positives increases with more broken channels. The other increase is due to an *efficiency trade-off* in the multiplicity channels. This is best illustrated with the TDR method in Fig. 6. In that case, when the number of broken channels increases all counts will move towards the bottom-left, towards the cut of a lower multiplicity. In the case of an event with multiplicity two there is an efficiency loss due to counts moving from a multiplicity of two to a multiplicity of one. There can also be an efficiency gain from previously wrong Multiplicity Predictions of events with an assigned multiplicity of three or higher. Their counts will move from above the cut for multiplicity two into the cut for with a multiplicity two. This effect will be referred to as an efficiency trade-off.

For the DNN detector efficiency the efficiency trade-off is the cause for an increase in efficiency for events with a multiplicity of two to four. This efficiency trade-off is most severe with events with multiplicity of four. In that case there is an efficiency increase of 1.8% with the DNN method at 20% broken channels and for the restricted efficiency there is an increase of 1.2%. This efficiency gain can be explained by looking at the Multiplicity Efficiency of events with a multiplicity of five. Here the DNN performance is most severely affected by the effect broken channels. The DNN efficiency decreases with 10.5%. Therefore, the neutron-multiplicity five is most affected which is the cause of an efficiency gain for the events with a multiplicity of four. Keep in mind that in the case of events with a multiplicity five it is most probable that there will only be an efficiency loss because at a multiplicity of five, gain from higher multiplicities exists. In addition to the efficiency trade-off it is also plausible that the efficiency leak is limited because of the same reason as with the TDR method. The DNN also uses the number of clusters as an input. The number of clusters is equal for both methods. The same reasoning can be applied to why this limits the efficiency loss to lower multiplicities. However, one of the consequences of a DNN is that there is limited knowledge on why and how it makes a prediction. Likewise, it cannot be explained with absolute certainty how a DNN behaves in the case of broken channels.

3.1.2 Hit Selection

The most important step in the Hit Selection is finding the right primary cluster. From the primary cluster it will be the signal with the shortest time-of-flight which will be labeled as the *showerhead*. Based on the *showerhead*, a four-momentum can be constructed from the neutrons time-of-flight and the distance traveled between the target and the position in the scintillator [11]. An invariant mass (inv. mass) spectrum can be constructed by using the four-momentum vectors of the neutrons. Equation 4 shows the inv. mass of an event with a multiplicity of n. As can be seen in Eq. 4 the inv. mass is dependent on the corresponding angle between the neutrons − the larger the angle the bigger the inv. mass. Within the inv. mass spectra it will only be the correct Multiplicity Predictions which will be counted in the inv. mass spectrum. From the difference in mass between the inv. mass of n free neutrons and the inv. mass obtained in Eq. 4 an inv. mass difference spectrum can be obtained (shown in Fig. 11). This shifted inv. mass spectrum will be denoted as the inv. mass difference spectrum. In order to compare to other literature studies [14], the choice has been made to look at events with a multiplicity of four in order to be able to do a comparison in performance. In Fig. 11 the inv. mass difference spectra with the DNN method can be seen for neutron energies of 200, 600 and 1000 MeV with twelve double planes.

$$M_{inv}^2 = (\sum_{i=1}^{n} E_i)^2 - |\sum_{i=1}^{n} \vec{\mathbf{p}}_i|^2 \tag{4}$$

Besides the physics list uncertainties (explained in Sect. 2.6) the simulations also contain statistical uncertainties. These statistical uncertainties consist of a Poisson uncertainty and an uncertainty in the initialization of the training. When starting with the training for the DNN the weights are given as random numbers. Starting with these numbers the training is optimized by using a minimization function. However, since the training is performed with a finite number of iterations the outcome of the minimization procedure will not give the some DNN. Thus, the initialization procedure plays a role in the statistical uncertainty. The statistical uncertainty has been studied in [14] and it was concluded that the statistical uncertainty decreases when a higher number of double planes are used. However, the study was done with four-neutron events. Therefore, the statistical uncertainty due to the initialization procedure has not yet been quantified for two-neutron events.

Broken channels are expected to have an effect on the invariant mass spectrum. In the most intuitive case, it can happen that the *showerhead* that is used for the neutron reconstruction is lost. This has a direct impact on the inv. mass spectrum, because another signal will have to be labeled and used as the *showerhead*. On a broader scale the number of counts will be effected. A count will only be shown in the inv. mass spectrum if the correct multiplicity is predicted for the event. As shown in Sect. 3.1.1 broken channels have an effect on the events with a multiplicity of four. For the analysis two data sets will be looked at: the total number of counts of the inv. mass spectra and the total number of count for the interval $[0-1]$ MeV. The total number of counts between $[0-1]$ MeV will be referred to as *peak count*. The Poisson distribution is given by $\sqrt{n}$ in the expected accuracy for the total count and *peak count*, where n is the number of counts.

In Fig. 11 the inv. mass spectra is seen for 200, 600 and, 1000 MeV neutrons. The results for 200 MeV behave intuitively as expected: with increasing percentage of broken channels the total number of counts and *peak count* drop. This is due to the drop in Multiplicity Efficiency. However, at 600 and 1000 MeV the same trend cannot be observed. At 600 MeV with 20%

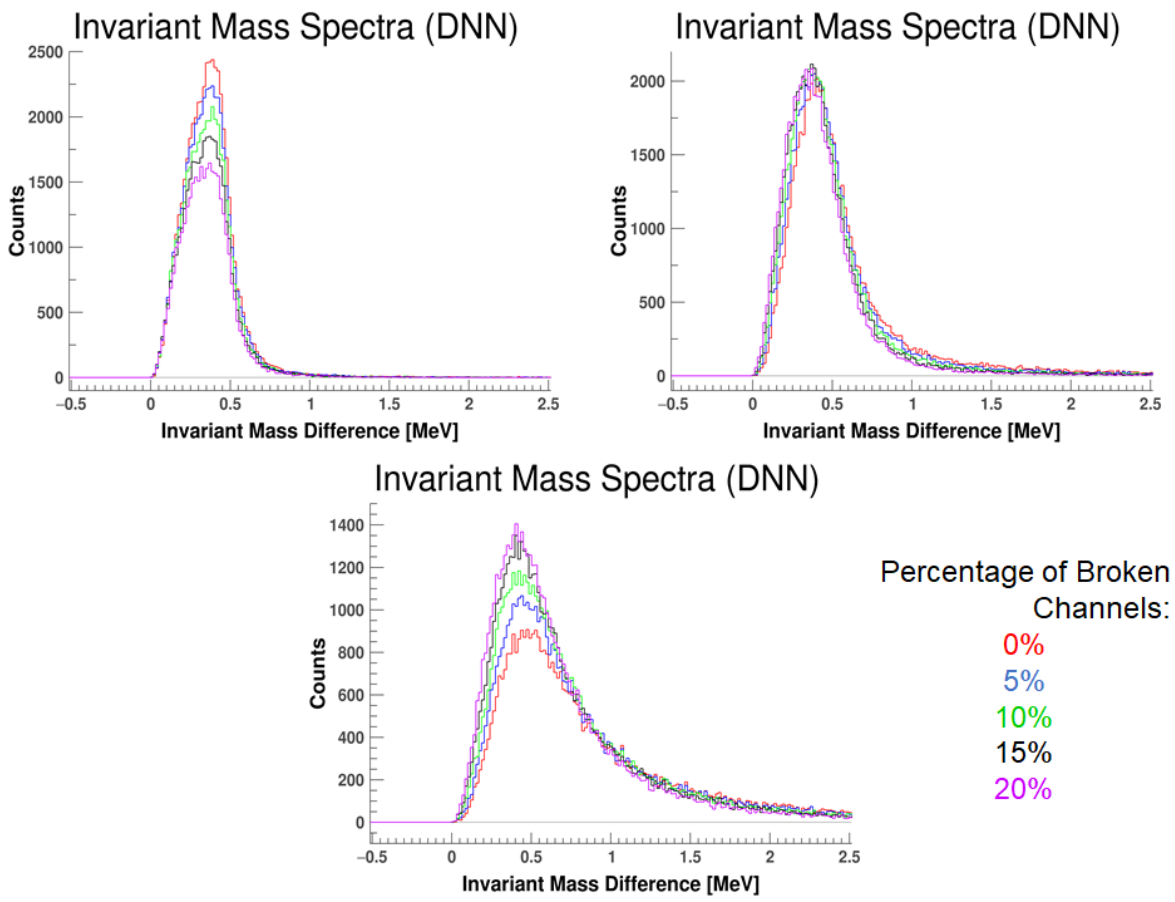

Figure 11: Invariant Mass Difference Spectra of the DNN method for 200 (top left), 600 (top right) and 1000 (bottom) Mev plotted for different percentages of broken channels between $0 - 20\%$ with increments of 5%, with twelve double planes.

broken channels the *peak count* increases with roughly 1.5% (See Appendix. Table 11). The inv. mass peak shows to have an increase in efficiency when scintillator bars are turned off. The same effect can be seen with 1000 MeV. In this case the *peak count* has an increase of roughly 43% (See Table 1).

In Table 1 the total number of counts in the invariant mass spectrum is shown for 1000 MeV with the DNN method. This was found by taking the integral underneath the curve of the inv. mass spectra (Fig. 11). In the first column the percentage of broken channels is given. The second and third column show the total number of counts and *peak counts* respectively. The fourth column shows the ratio between the *peak count*, and the total number of counts. The fifth and final column shows the increase/decrease of the *peak count*. This was done by finding the ratio of the number of *peak counts* with broken channels to *peak count* with no broken channels (the first row).

From Table 1, it can be seen that with neutron energies of a 1000 MeV with events of multiplicity-four both the total number of counts and *peak count* increases with a higher percentage of broken channels. From the fourth column, it can be observed that the accuracy of the DNN increases and that a higher percentage of counts lie within $[0 - 1]$ MeV.

The reason why the four-neutron invariant mass spectrum was selected was to be able to

B.C. [%]	Total Count	Peak Count	% Peak	Ratio Peak
0	45322	30396	67	1.00
5	48503	34815	72	1.15
10	50967	38607	76	1.27
15	52557	41315	79	1.36
20	53400	43606	82	1.43

Table 1: The counts obtained from the four-neutron inv. mass spectra with 1000 MeV and twelve double planes - DNN Method, Stochastic Shut-Off Scenario.

do a comparison with existing data. However, one might ask if it is even accurate to draw conclusions from an inv. mass data analysis for four-neutron events with twelve double planes. The ratio of (DNN efficiency of restricted multiplicity) / (DNN multiplicity) for 200, 600 and 1000 MeV with 20% broken channels is 0.50, 0.51 and 0.53 respectively. Roughly half of the Multiplicity Predictions for four neutron events is a false positive. This issue is further enforced in the paper by C. A. Douma [14]. With twelve double planes, the largest multiplicity that has an acceptable fraction of false positive events ($< 25\%$) is with two neutrons. For events with a multiplicity of three, sixteen double planes are required, for four neutrons at least 23 needed and for five neutrons, the required number of double planes is 30 [14]. Therefore, in order to further study the effect of inv. mass accuracy at 1000 MeV a new simulation was performed. In this case, the inv. mass spectrum of two-neutron events was analysed.

B.C. [%]	Total Count	Peak Count	% Peak	Ratio Peak
0	73972	68603	93	1.00
5	74388	70016	94	1.02
10	74338	70626	95	1.03
15	74243	70974	96	1.03
20	73597	70721	96	1.03

Table 2: The counts obtained from the two-neutron inv. mass spectra with 1000 MeV and twelve double planes - DNN Method, Stochastic Shut-Off Scenario.

In Table 2 the inv. mass count is shown for events with a multiplicity of two with the DNN method. In order to take out the false-positives, a first approximation was used based on the percentage of false-positives that were found in the DNN and DNN restricted multiplicities (Appendix Fig. 16 - 35). The number of counts for neutron multiplicity-two was multiplied by (DNN restricted)/(DNN). In Table 3 the same information can be found for the TDR method. The same first approximation for the false-positives was applied for the TDR method, but here the multiplicity efficiencies of the TDR and TDR restricted were used.

When looking at the total number of counts both methods show an increase in Multiplicity Efficiency. The increase in Multiplicity Efficiency is due to the effect of an efficiency trade-off (explained in Sect. 3.1.1). Not only does the total number of counts increase, the *peak count* also shows an increase for both the TDR and the DNN method with increasing number of broken channels. This increase is partly because the *peak count* percentage gets larger, implying that more *showerheads* are chosen that are closer to the beam. When *showerheads* are chosen that are closer to the beam their corresponding angle should decrease, thus reducing the inv. mass.

B.C. [%]	Total Count	Peak Count	% Peak	Ratio Peak
0	36266	27598	76	1.00
5	37253	28895	78	1.05
10	37895	29783	79	1.08
15	38494	30494	79	1.10
20	38992	31053	80	1.12

Table 3: Same as Table 2 but for TDR method.

At 20% broken channels the DNN has an increase in *peak counts* of 3.1% and the TDR 12.5% respectively. This can give the impression that there is an increase in efficiency with more broken channels. However, in the case of broken channels, more and more clusters will either split up or will lose signals. This has an effect on which primary clusters are chosen. When looking at how the primary clusters are chosen for the TDR method (Eq. 3) it can be seen that clusters with a higher energy deposit will have a lower *R-Value*. But since a cluster will either split up or have a decrease in energy deposit the correct primary clusters will become less distinct. Consequently, with energy deposit of primary clusters becoming less distinctive it will be the cluster velocity which will have a more predominant effect when finding primary clusters (Eq. 3). As a consequence the Hit Selection of the TDR method will choose more signals that are closer to the beam, thus improving the resolution of the inv. mass difference. This effect can be seen in Fig. 12. With increasing percentage of broken channels it can be clearly seen that the TDR method chooses *showerheads* that are closer to the beam. However, this increase in efficiency does not imply that the full neutron reconstruction becomes more accurate and should be seen as an artifact of the way the reconstruction is done.

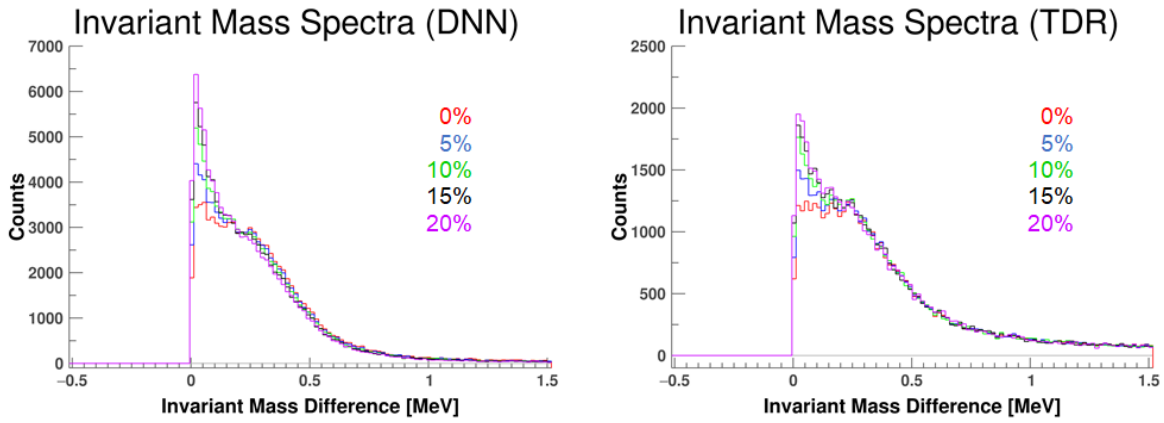

Figure 12: Invariant Mass Difference Spectra of the DNN (left) and TDR (right) method for 1000 MeV two-neutron events with different percentages of broken channels between $0 - 20\%$ with increments of 5%, with twelve double planes, Stochastic Shut-Off Scenario.

Similar to the TDR method the DNN method also shows an increase in *peak count*. When looking at Fig. 12 the same conclusion can be drawn as to why there is an increase in *peak counts*. With increasing percentage of broken channels the DNN chooses signals that are closer to the beam, because the primary clusters become less distinct. This can be understood by looking at how the DNN chooses a primary clusters (see Sect. 2.5.2). A DNN is trained to distinguish primary and secondary clusters, however, because these clusters become altered

they will not consist of the same cluster properties that distinguishes primary from secondary clusters. Therefore, in the case of broken channels, out of the remaining altered clusters, the DNN will favour clusters with signals with a shorter time-of-flight [23], thus increasing the *peak count*.

When looking at Fig. 12 it can be seen that there is a shift in the inv. mass for events possessing a higher inv. mass difference to energies which lie in the range $[0 - 0.1]$ MeV. As explained above this is because the DNN will favour choosing signals that are closer to the beam to be the *showerhead*. Because these *showerheads* lie closer to the beam their corresponding angle between the two *showerheads* decreases, thus decreasing the inv. mass (See Eq.4). The total number of counts between $[0 - 0.1]$ MeV can be seen in Table 4 for the DNN method.

B.C. [%]	Total Count $[0 - 0.1]$ MeV	Ratio Count $[0 - 0.1]$ MeV
0	18778	1.00
5	22331	1.19
10	25261	1.35
15	27584	1.47
20	29844	1.59

Table 4: The counts obtained from the two-neutron inv. mass spectra between $[0 - 0.1]$ MeV with 1000 MeV and twelve double planes - Stochastic Shut-Off Scenario, DNN method.

In Table 4, the first column shows the percentage of broken channels, the second column shows the total number of counts of events calculated to have an inv. mass between $[0 - 0.1]$ MeV, and the last column shows the ratio of total number of counts similar to Table 2. From Table 4, it can be seen that already at 5% broken channels there is a shift in the inv. mass, favouring signals that correspond to an inv. mass between $[0 - 0.1]$ MeV. At 5% this effect corresponds to an increase in the total number of counts of 18.9%. This shift in the inv. mass counts results in an increase in the total number of counts of 58.0% at 20% broken channels.

3.2 Worst-Case Scenario

When an experiment is done with the NeuLAND detector, every detector has an equal chance of becoming 'broken'. This means that it is possible that bad luck strikes and the most crucial detectors will break down simultaneously. This scenario will be referred to as the *Worst-Case Scenario*. In this scenario the detectors that will be shut off will go in descending order starting with the most crucial detector. During an experiment this might force the researchers to stop the beam time and repair the detector due to an unacceptable efficiency loss instead of continuing the experiment. However, this scenario raises two questions: which scintillator bars are the most crucial? And how critical are these detectors in the overall performance? The simulation is done at 600 and 1000 MeV and is similar to the method used in 3.1.

3.2.1 Most Crucial Channels

The question of which scintillator bars are the most crucial ones was answered based on three different observables: the channel with the largest number of signals, the channel with the largest number of *showerheads*, or the channel with the most deposited energy. The detector with the largest number of *showerheads* has the most direct impact on the four-momentum reconstruction, as the reconstruction has to be done with other signals. Therefore, it was

assumed that this would have to the most significant impact on the inv. mass spectra. In order to test this assumption it was compared to the channel with the largest number of energy deposit and the largest number of signals. These answers are based on the results of one million simulated events. Based on the simulated data all the detectors can be ordered in descending order based on importance of total energy deposit, number of *showerheads*, and number of singals. The total number of counts obtained from the inv. mass spectra can be seen in Table 5 for Total Signals (T), Number of *showerheads* (S), and Total Energy Deposit (E). The inv. mass spectra is obtained from events with a multiplicity of four. The simulation was done with one million events. The precentage broken channels was between $(0 - 4\%)$ with increments of 1%, which is equal to twelve channels. For each simulation the channels that were turned off were based on the the most crucial channel for each category.

B.C. [%]	Peak Count (T)	Peak Count (S)	Peak Count (E)
0	48790	48790	48790
1	49302	47265	48890
2	46199	41328	46631
3	40054	35549	40231
4	35217	29744	35657

Table 5: The Peak Count obtained from the two-neutron events with broken channels according to: Total Signals (T), *showerheads* (S) and Energy Deposit (E) with 600 MeV and twelve double planes - DNN Method.

Table 5 shows that the detectors with the largest number of *showerheads* are the most crucial detectors. The drop in *peak count* was far more severe when the most crucial channels in the category *showerhead* were shut off compared to the detectors based on total number of signals and total energy deposit. Conceptually, this makes the most sense. The *showerhead* signals are the signals that are used for neutron reconstruction. In the case that these signals are lost the DNN has to use other signals for the neutron reconstruction and thus the inv. mass spectrum is most severely impacted. When looking at the position of the most crucial channels for each of the three scenario's. From the gathered data the two most central detectors of the first plane had the largest number of *showerheads*, followed by the two most central detectors of the second plane. For the categories total number of counts and energy deposit, the most crucial channel was in the fourth double plane. The chance of the *showerhead* being closest to the beam is highest for the channels in the first double plane. Even at 4% broken channels there were no detectors from the first double plane included for total number of signals and energy deposit.

3.2.2 Broken Modules Scenario

Based on the results depicted in Sect. 3.2.1, a Worst-Case Scenario has been implemented. In Neuland, all channels are broken down in groups of eight [12]. All channels are grouped in eight per electronic module and these electronic modules are the ones that can break down during an experiment [10]. Due to lack of CPU time, the most crucial modules were chosen based on the importance of the most crucial individual channels. The module that held the most crucial channel would be characterised as the most crucial module. If the second most crucial channel is already in the first most crucial module than the channel after that is picked for the second most crucial model, etc. The data analysis of the Worst-Case Scenario was done with 600 MeV with twelve double planes and a total of one million simulated events. For the Worst-Case Scenario the Multiplicity Efficiency and the inv. mass difference will be studied. For the inv.

mass only the events with multiplicity of two will be considered. The effect of broken modules was tested up to three broken modules.

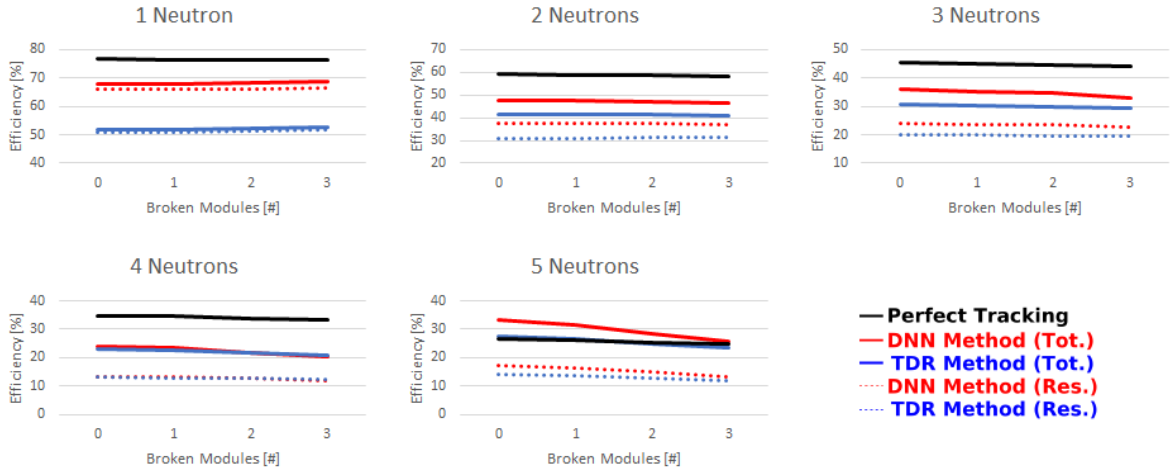

Figure 13: Detector Efficiency for various neutron multiplicities with 600 MeV and twelve double planes for the realistic Worst-Case Scenario.

In Fig. 13 the Multiplicity Efficiency can be seen for the realistic Worst-Case Scenario. One module equals eight scintillator bars. The first module was located in the centre of the first plane, the second module in the centre of the second plane, and the third in the third plane. For events with a multiplicity of one there is a small increase in efficiency with two and three broken modules. This is due to the same behaviour as the increase for the TDR method with events with a multiplicity of one events explained in Sect. 3.1. At higher neutron multiplicities there is a steady decrease in efficiency with a higher number of broken channels. As expected the efficiency drop is more significant for higher neutron multiplicities. Events with a multiplicity of five show the most severe decrease in efficiency with a drop of 7.6% with three broken modules. Events with a multiplicity of two to four show an efficiency drop with 3 broken modules of 1.3%, 2.9%, and 3.6% respectively.

B.M. [#]	Total Count	Peak Count	% Peak	Ratio Peak
0	75087	73794	98	1.00
1	74641	73242	98	0.99
2	74115	72653	98	0.98
3	73789	72237	98	0.98

Table 6: The counts obtained from the two-neutron inv. mass spectra with 600 MeV and twelve double planes - DNN Method, Realisic Worst-Case Scenario.

In Tables 6 and 7 the inv. mass count and *peak count* can be seen for the realistic Worst-Case Scenario for two-neutron events with the DNN and TDR methods. Both the total number of counts and *peak count* decrease for multiplicity-two events with increasing number of broken modules. The *peak counts* shows with one broken module a decrease of 1.0% for the DNN and 1.0% for the TDR method. This grows to 2.1% and 4.0% with three broken modules, respectively. The DNN method does not show a decrease in percentage of counts that lie

B.M. [#]	Total Count	Peak Count	% Peak	Ratio Peak
0	48560	39155	81	1.00
1	48242	38615	80	0.99
2	47999	38091	79	0.97
3	47727	37599	79	0.96

Table 7: Same as Table 6 but for the TDR method.

between [0-1] MeV. From this, it can be concluded that when the correct *showerhead* signals are lost the DNN still favours signals that lie close to the beam.

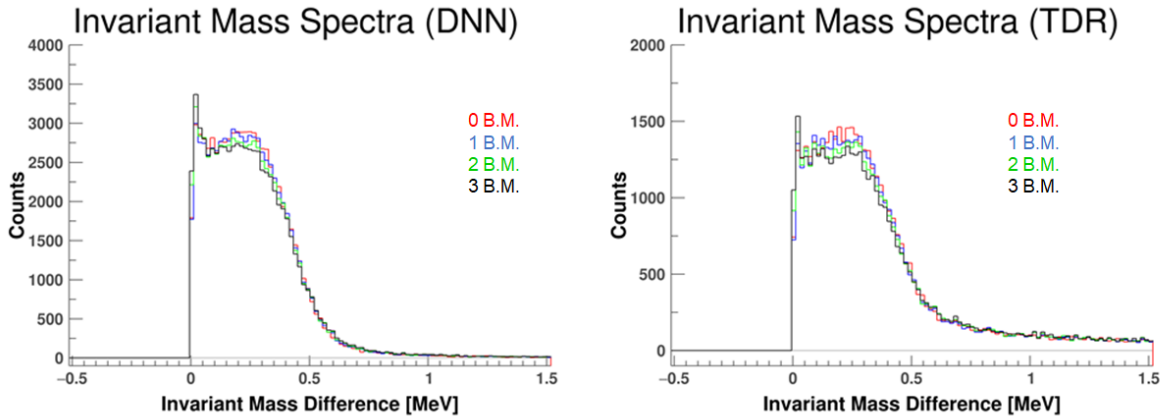

Figure 14: Invariant Mass Difference Spectra of the DNN (left) and TDR (right) method for 600 MeV two-neutron events with different percentages of broken modules between $0-3$ with increments of 1 module, with twelve double planes, Realistic Worst-Case Scenario.

When looking at Fig. 14 a similar effect can be seen as with the inv. mass spectrum of the Stochastic Shut-Off Scenario (Fig. 12). In the case of broken modules and the correct *showerhead* signals are lost both the DNN and the TDR method still favour signals that lie close to the beam (as explained in Sect. 3.1.2). This effect can be seen in Table 8.

B.M. [#]	Total Count $[0-0.1]$ MeV	Ratio Count $[0-0.1]$ MeV
0	15926	1.00
1	15546	0.98
2	16318	1.02
3	16758	1.05

Table 8: The counts obtained from the two-neutron inv. mass spectra between $[0-0.1]$ MeV with 600 MeV and twelve double planes - Worst Case scenario, DNN.

Similar to Table 4, Table 8 shows the increase/decrease of the total number of counts between $[0-0.1]$ with the DNN method. In this case it is tested with increasing number of broken modules and with 600 MeV. With one broken module there is a decrease of 2.4%. This decrease is higher than the decrease in the *peak count* with one broken module shown in Table 6, even when taking the error margins into account. This implies that already at one broken

module there is shift in the calculated inv. mass for multiplicity-two events. With two and three broken modules there is an increase in the total number of counts between $[0 - 0.1]$ MeV of 2.5% and 5.2%, respectively.

3.2.3 Comparison between the Stochastic and Worst-Case Scenarios

In both the Stochastic Shut-off and the Worst-Case Scenarios the percentage/number of broken channels was chosen in order to show the performance of the DNN. The starting number of broken channels was equal to sixty channels (5%) for the Stochastic Shut-Off Scenario, whereas for the Worst-Case Scenario eight channels (corresponding to one module) were used. However, in order to accurately compare both scenarios an additional simulation was performed. This simulation was performed with 1000 MeV and twelve double planes. The modules that were turned-off were chosen according to the principle explained in Sect. 3.2.1. This simulation was performed with up to eight broken modules, with increments of two broken modules. Similar to the Stochastic Shot-Off Scenario a first approximation was applied to the total number of counts (Appendix Fig. 36 - 45). The total number of counts is shown in Table 9 and depicted in Fig. 15.

B.M. [#]	Total Count	Peak Count	% Peak	Ratio Peak
0	76497	68296	89	1.00
2	76153	68063	89	1.00
4	74529	66295	89	0.97
6	71570	64214	90	0.94
8	69148	61767	89	0.90

Table 9: The counts obtained from the two-neutron inv. mass spectra with 1000 MeV neutrons and twelve double planes - DNN Method, Worst-Case Scenarios.

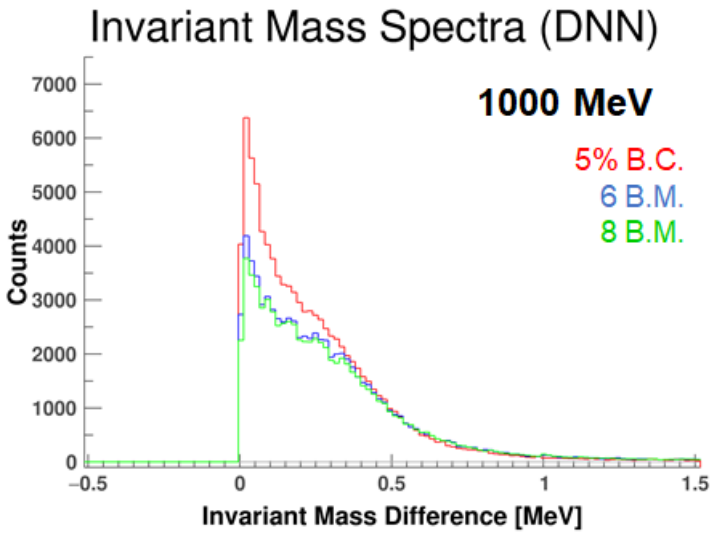

Figure 15: Multiplicity two-events with 1000 MeV and twelve double planes - DNN method, comparison of the Stochastic Shut-Off and Worst-Case Scenarios.

Five percent of broken channels which equals to 60 detector elements is in between 6 and 8

broken modules (48 and 64 detector elements, respectively). From Table 2 it can be seen that for 5% broken channels there is an increase of 2.1% for the total number of *peak counts*. However, from Table 9 it can be seen that at both six and eight broken modules there is a decrease in *peak count*. This decrease is equal to 6.0% and 10.0%. This difference in *peak count* is clearly illustrated in Fig. 15. From the results shown in Table 9 and Fig. 15 it can be concluded that it does in fact matter which channels are broken down and that the Worst-Case Scenario shows a bigger loss in efficiency compared to the Stochastic Shut-Off Scenario. This is plausible as for the Worst-Case scenario, channels were chosen which were closer to the beam making them more crucial for event reconstruction.

4 Discussion

In the present study, the effect of broken channels on the NeuLAND performance was studied by looking at the efficiency of the Multiplicity Predictions and the inv. mass spectrum. First, a Stochastic Shut-Off was studied with neutron energies of 200, 600 and 1000 MeV. The Stochastic Shut-Off Scenario was studied by turning off a percentage of channels, which were chosen randomly for each single event. Then, a Worst-Case Scenario was proposed based on the number of the *showerheads* in a single channel with neutron energies of 600 and 1000 MeV. For the Worst-Case Scenario the same module(s), consisting of eight detectors stacked next to each other, was (were) turned off throughout the whole simulation. All simulations were done with twelve double planes. In order to assess the importance of the most crucial channels a comparison was made between the Stochastic Shut-Off and Worst-Case Scenario based on the inv. mass spectrum of events with a multiplicity of two and neutron energies of 1000 MeV.

The Stochastic Shut-Off Scenario was tested with $0-20\%$ broken channels with increments of 5%. The Multiplicity Efficiency at 200 MeV was in line with the expectation for this scenario. As expected the DNN showed a decrease in efficiency in the case of broken channels for all neutron multiplicities and broken channel percentages. The TDR showed similar results, except for events with a multiplicity of one. This is a logical consequence of the initialization of the TDR method. The TDR only loses efficiency for events with a multiplicity of one in the case that all signals are lost. Simultaneously, wrong predictions with higher multiplicities will cause an efficiency gain for multiplicity-one events. When looking at 600 MeV neutrons the same trend was found only with the difference that the decrease in efficiency was lower compared to 200 MeV events, for both the TDR and DNN. At 1000 MeV there was an increase in efficiency in the Multiplicity Determination for events with multiplicity two to four with the DNN method. This was due to an efficiency trade-off between the Multiplicity Determinations.

There are limitations to the conclusions that can be made from the Multiplicity Determination. One such limitation is clearly seen when looking at the 1000 MeV Multiplicity Determination with the TDR method. When comparing Figs. 8 - 10 it can be seen that at 1000 MeV the efficiency loss is less severe for the TDR and DNN methods compared to lower energies. For the TDR method, it was concluded that this phenomenon stems from the effect that broken channels has on the number of clusters. The number of clusters either grows or decreases more slowly compared to 200 and 600 MeV events. As the number of clusters is also used as an input for the DNN method this effect must also be present. From this it can be concluded that there is a significant alteration on the cluster properties with increasing number of broken channels. However, the significance that the alteration in cluster properties has on the Multiplicity Determination is unclear because the internal structure of DNN cannot be easily investigated.

With the Stochastic Shut-Off at 1000 MeV the Hit Selection showed an increase in efficiency for both the DNN and the TDR methods. In the case of events with a multiplicity of two there was an increase of 3.2% and 12.5% at 20% broken channels, respectively. However, this increase in efficiency does not imply that the obtained inv. mass spectrum is more reliable. From Fig. 12 it can be concluded that in the case of broken channels both methods predominantly choose signals that are closer to the beam to be a *showerhead*. These signals are not necessarily the correct *showerheads*. Appointing primary clusters, and thus selecting the *showerhead*, is done with a DNN. As was concluded from the Multiplicity Efficiency there is a significant alteration in the cluster properties. Based on the difference in cluster properties the DNN can distinguish primary from secondary clusters, however with altered clusters this distinction becomes less

distinctive. Consequently, the DNN will favour clusters that lie closer to the beam. This effect can clearly be seen when looking at Table 4. The increase in *peak count* is not in the same range as the increase in total number of counts between $[0 - 0.1]$ MeV. The conclusion is that the efficiency using the inv. mass spectrum does not solely reflect the accuracy of a full neutron reconstruction as the events shift in this spectrum when one experiences broken channels.

The Worst-Case Scenario was studied by turning off the most crucial modules with neutron energies of 600 and 1000 MeV. From Table 5, it is concluded that the category *showerheads* contained the most crucial channels. Only this category was used when studying the Worst-Case Scenario due to lack of CPU. A comparison was made between the Stochastic Shut-Off and Worst-Case Scenarios with neutron energies of 1000 MeV. Fig. 15 shows that it does in fact matter which channels are turned-off because the efficiency due to turning off the most crucial modules is significantly lower. Intuitively, this makes sense, because with the Stochastic Shut-Off Scenario, channels that barely contained any signals were also turned-off. Contrary to this, in the Worst-Case Scenario the channels that were turned-off contained the most *showerheads*, thus directly influencing the inv. mass spectrum.

For neutron energies of 600 MeV, the DNN shows a decrease of 1.0% in the *peak count* with one broken module and a multiplicity of two. With two and three broken modules the decrease grows to 2.1% and 4.0%, respectively. In addition to this decrease in efficiency it is seen in Table 8 that there is an internal shift in the inv. mass spectrum. At one broken module there was a decrease in counts between $[0 - 0.1]$ MeV of 2.4%. At two and three broken modules there was an increase of 2.5% and 5.2% in the same range, respectively.

From this, it is concluded that when performing experiments on finding nuclear cross sections, with multiplicity-two events and neutron energies of 600 MeV, the effect of broken channels will not pose a problem when the inv. mass resolution of the apparatus is 0.6 MeV or larger. Up to a resolution of 0.6 MeV only a a decrease in efficiency can be observed. This only forces the researcher to prolong the experiment in order to obtain the same number of data. Although the efficiency loss is shown to be small. However, with a higher accuracy in the resolution the internal shift in the inv. mass spectrum, reflected in Table 8, will effect the acquired data, causing the obtained inv. mass spectrum to be unreliable. The resolution found in this study is not applicable for experiments with other neutron energies, and events with a different neutron multiplicity. From the Stochastic Shut-Off Scenario (Fig. 11) it was concluded that the inv. mass spectrum vastly differs with different neutron energies in the case of broken channels. Similarly, when increasing the neutron multiplicity the inv. mass spectrum will directly be influenced. As shown in Eq. 4 the inv. mass is dependent on the mutual angle of the neutrons. With more neutrons the inv. mass will generally be larger. Therefore, studies have to be done for each measurement to find out up to what the resulting energy resolution will be.

From the results shown in Ref. [14] experimental data are roughly between the physics lists of QGSP_INCLXX_HP and QGSP_BERT_HP. Therefore, additional studies can be done on the systemic errors when one analysis the performance of NeuLAND in the case of broken channels. From the same study it was found that the initialization for training the DNN method showed that sixteen double planes are needed to do accurate measurements of the inv. mass spectrum of events with a multiplicity of four. However, in this study the main focus was on multiplicity-two events. The statistical errors due to the initialization of the training of the DNN has not yet been studied for multiplicity-two events. In order to properly assess the statistical uncertainty in the performance of the DNN additional studies have to be done for multiplicity-two events.

5 Conclusions

With the use of simulated data the effect of broken channels on the performance of the NeuLAND detector was studied. The studies were made by analysing and comparing the Multiplicity Efficiency and the inv. mass spectrum using the DNN method. As the DNN method is still a relatively new method for NeuLAND, the already existing caliometric TDR method was used for verification. The results were compared by using the data generated for one million events. The detector used consists of twelve double planes. The final design goal of NeuLAND is to have 30 double planes.

As a first approximation a Stochastic Shut-Off Scenario was investigated. The Stochastic Shut-Off Scenario was studied by turning off a percentage of the channels, which were chosen randomly for each simulated event. The percentage of broken channels was varied in the range $0 - 20\%$ with increments of 5%. The multiplicity performance of 200 and 600 MeV showed a decrease in efficiency with a neutron multiplicity of one to five with the DNN method. At 1000 MeV the DNN method showed an increase in efficiency for events with a neutron multiplicity of one to four. This was partly due to an efficiency trade-off between multiplicity channels. However, the multiplicity performance did not show the effect of broken channels on cluster properties. From the TDR method, it was concluded that at 1000 MeV the number of clusters increased or decreased more slowly with increasing percentage of broken channels when compared to neutron energies of 200 and 600 MeV. Therefore, conclusions made about the effect of broken channels on the DNN Multiplicity Efficiency remain limited.

The effect of broken channels on the inv. mass spectrum with the Stochastic Shut-Off Scenario was done by looking at neutron multiplicity-two events with 1000 MeV. The DNN method showed an increase of 3.1% for the *peak count* at 20% broken channels. This increase in efficiency does not imply that the full neutron reconstruction becomes more accurate and should be seen as an artifact of the DNN method. The Multiplicity Efficiency does not fully reflect the accuracy of the full neutron reconstruction. When looking at the inv. mass spectra (Fig. 12 and Table 4) it can be seen that in the case of broken channels the *showerheads* chosen lie closer to the beam. This is because the DNN used for the primary cluster determination distinguishes between primary and secondary clusters. In the case of broken channels the primary clusters become less distinct. Consequently, the DNN favors more the clusters that lie closer to the beam.

A second study was performed by investigating the effect of broken channels in the case when the most crucial channels are shut off. In order to find the most crucial channel a study was performed by turning off the most crucial channels based on three categories: the total number of signals, the total number of *showerheads*, and total energy deposited. It was concluded that the number of *showerheads* detected in a scintillator bar showed the most severe decrease in number of *peak counts*. As a Worst-Case Scenario the most crucial modules, eight detectors stacked right next to each other, were turned off during the simulation. The results of the simulations showed that the *peak count* decreases with 1.0% for the DNN with one broken module. With three broken modules the decrease grows to 2.1% and 4.0%, respectively. However, in addition to the change in the efficiency, an internal shift in the inv. mass spectrum was observed. At one broken module there was a decrease in the number of counts between $[0 - 0.1]$ MeV of 2.4%. However, at two and three broken modules there was an increase of 2.5% and 5.2%, respectively.

Therefore, it is concluded that when performing experiments on finding nuclear cross sections, with multiplicity-two events and neutron energies of 600 MeV, the effect of broken modules will not pose a problem with an energy resolution of about 0.6 MeV for the inv. mass spectrum. If the resolution is much better than 0.6 MeV for a certain multiplicity, when studying the effect of broken channels, one should be careful when using the inv. mass spectrum due to the internal shifts which are inherent in the way the neutron tracks are reconstructed.

References

[1] P. Spiller and G. Franchetti, The FAIR accelerator project at GSI, Nuclear Instruments and Methods in Physics Research Section A: Accelerators, Spectrometers, Detectors and Associated Equipment 561 (2006) Proceedings of the Workshop on High Intensity Beam Dynamics 305.

[2] GSI, NUSTAR/ENNA, URL: https://www.gsi.de/en/work/research/nustarenna.htm.

[3] GSI, The Super-FRS in the FAIR Project, URL: The Super-FRS Layout.

[4] GSI, A next generation experimental setup for studies of Reactions with Relativistic Radioactive Beams URL: R3B

[5] The R3B collaboration 2014 Technical Report for the Design, Construction and Commissioning of the Tracking Detectors for R3B Tech. rep. GSI Helmholtzzentrum fur Schwerionenforschung

[6] D. Cortina-Gil et al., CALIFA, a Dedicated Calorimeter for the R3B/FAIR, Nuclear Data Sheets 120 (2014) 99–101.
URL: http://www.sciencedirect.com/science/article/pii/S0090375214004694

[7] B. Gastineau et al., Design Status of the R3B-GLAD Magnet: Large Acceptance Superconducting Dipole With Active Shielding, Graded Coils, Large Fiorces and Indirect Cooling by Thermosiphon, Trans. on App. Supercond. 18 (2) (2008) 407–410.
URL: https://ieeexplore.ieee.org/document/4495518

[8] GSI, *The "Machine"*,
URL: https://www.gsi.de/en/researchaccelerators/fair/the_machine.htm.

[9] The R3B collaboration, Technical Report for the Design, Construction and Commissioning of NeuLAND: The High- Resolution Neutron Time-of-Flight Spectrometer for R3B, Tech. rep., GSI and Collaborators (2011).
URL: https://edms.cern.ch/ui/file/1865739/2/TDR_R3B_NeuLAND_public.pdf

[10] Email correspondence with Dr. Igor Gašparić and prof. dr. Nasser Kalantar-Nayestanaki.

[11] J. Mayer, Charting NeuLAND: Towards multi-neutron reconstruction with the New Large Area Neutron Detector and The virtual gamma-ray spectrometer G4Horus, Dissertation Universität zu Köln, 2018.

[12] The R3B Collaboration, Technical Report for the Design, Construction and Comissioning of NeuLAND: The High-Resolution Neutron Time-of-Flight Spectrometer for R3B.

[13] C.A.Douma, Investigation of background reduction techniques for the NeuLAND neutron detector, Nuclear Instruments and Methods in Physics Research Section A: Accelerators, Spectrometers, Detectors and Associated Equipment 930 (2019).

[14] C.A.Douma, Development of a Deep Neural Network for the Data Analysis of the NeuLAND Neutron Detector, (to be published, used with permission).

[15] LeCun, Y., Bengio, Y. & Hinton, G. Deep learning. Nature 521, 436–444 (2015). URL: https://doi.org/10.1038/nature14539

[16] S. Agostinelli et al., Geant4, Nuclear Instruments and Methods in Physics Research Section A: Accelerators, Spectrometers, Detectors and Associated Equipment, 506 (3) (2003) 250–303. URL: http://www.sciencedirect.com/science/article/pii/S0168900203013688

[17] D. Bertini, R3BRoot, simulation and analysis framework for the R3B experiment at FAIR, J. Phys. Conf. Series 331 (3) (2011) 032036. URL: https://iopscience.iop.org/article/10.1088/1742-6596/331/3/032036/pdf

[18] E. B. Hoemann, Neural Network analysis for NeuLAND & Radiation exposure at interventional radiology, MSc. thesis, University of Cologne (2019).

[19] M. Polleryd, Convoluted Events: Neutron Reconstruction using Neural Networks, Ph.D. thesis, Chalmers University of Technology (2017).

[20] D. Guest et al., Deep Learning and Its Application to LHC Physics, Annual Review of Nuclear and Particle Science, Science 68 (1) (2018) 161–181. URL: https://doi.org/10.1146/annurev-nucl-101917-021019

[21] F. Chollet et al., Keras, GitHub Repository. URL: https://keras.io/

[22] M. Abadi et al., TensorFlow: Large-Scale Machine Learning on Heterogeneous Distributed Systems, ArXiv, URL: http://arxiv.org/abs/1603.04467

[23] C. A. Douma, DNN module for R3BRoot. URL: https://github.com/R3BRootGroup/NeuLAND_DNN.git

[24] J. Schmidhuber, Deep learning in neural networks: An overview, Neur. Netw. 61 (2015) 85–117. URL: http://www.sciencedirect.com/science/article/pii/S0893608014002135

[25] J. Duchi et al., Adaptive Subgradient Methods for Online Learning and Stochastic Optimization, J. of Mach. Learn. Res. 489 12 (2011) 2121–2159. URL: http://www.jmlr.org/papers/volume12/duchi11a/duchi11a.pdf

[26] Z. Szabo et al., Cross-Entropy Optimization for Independent Process Analysis, ICA 2006: Independent Component Analysis and Blind Signal Separation, Sep. (2006) 909–916. URL: https://link.springer.com/chapter/10.1007%2F11679363_113

[27] C. A. Douma, Measurement of the Gamow-Teller states in ^{116}Sb and ^{122}Sb, PhD thesis, University of Groningen (2019).

6 Appendix

B.C. [%]	Total Count	Peak Count
0	48547	47947
5	45506	44985
10	41781	41334
15	38506	38135
20	34725	34361

Table 10: The counts obtained from the four-neutron inv. mass spectra with neutron energies of 200 MeV and twelve double planes - DNN Method, Stochastic Shut-Off Scenario, including false positives.

B.C. [%]	Total Count	Peak Count
0	56781	50078
5	56625	51566
10	56066	52176
15	55013	51985
20	50836	50836

Table 11: The counts obtained from the four-neutron inv. mass spectra with neutron energies of 600 MeV and twelve double planes - DNN Method, Stochastic Shut-Off Scenario, including false positives.

B.C. [%]	Total Count	Peak Count
0	92607	85886
5	94045	88518
10	94912	90172
15	95540	91332
20	95715	91975

Table 12: The counts obtained from the two-neutron inv. mass spectra with neutron energies of 1000 MeV and twelve double planes - DNN Method, Stochastic Shut-Off Scenario, including false positives.

B.C. [%]	Total Count	Peak Count
0	47731	36323
5	48954	37971
10	49601	38983
15	50225	39788
20	50554	40261

Table 13: The counts obtained from the two-neutron inv. mass spectra with neutron energies of 1000 MeV and twelve double planes - TDR Method, Stochastic Shut-Off Scenario, including the false positives.

B.C. [#]	Total Count	Peak Count
0	92875	82918
2	91544	81819
4	88716	78914
6	84564	75873
8	81539	72835

Table 14: The counts obtained from the two-neutron inv. mass spectra with neutron energies of 1000 MeV and twelve double planes - DNN Method, Worst-Case Scenario, including the false positives.

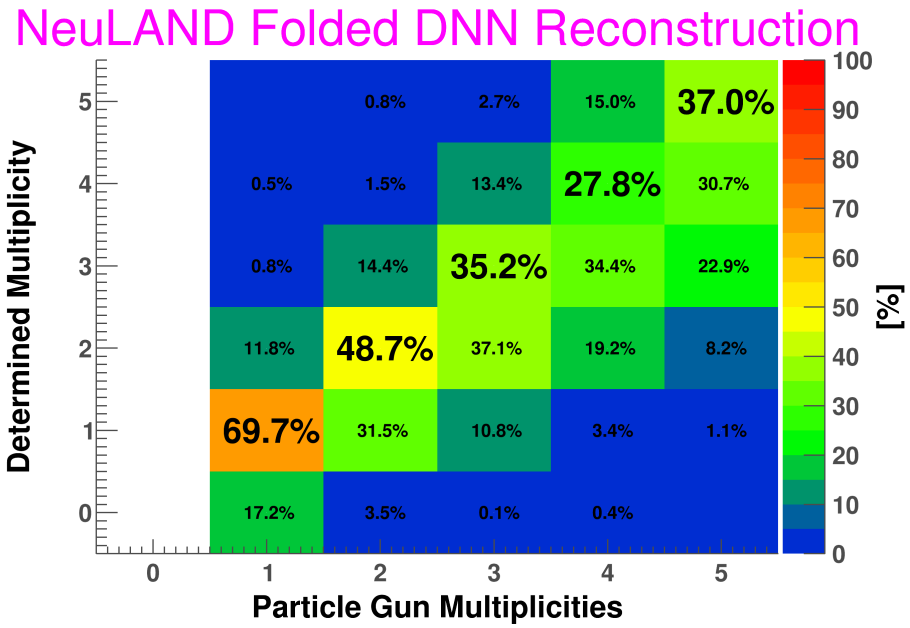

Figure 16: The obtained Multiplicity Prediction with two-neutron events and neutron energies of 1000 MeV and twelve double planes - 0% B.C. DNN method, Stochastic Shut-Off Scenario.

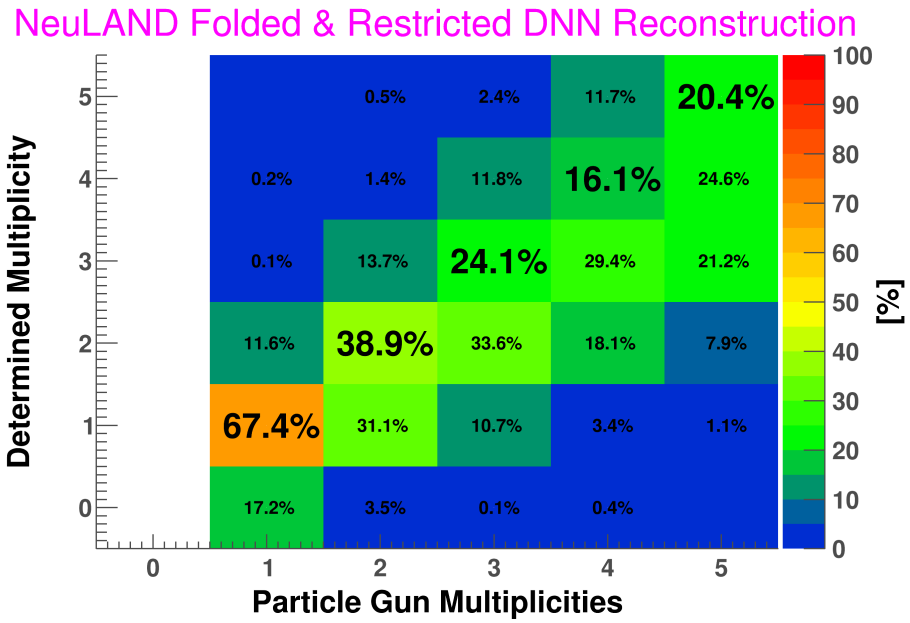

Figure 17: The obtained Multiplicity Prediction with two-neutron events and neutron energies of 1000 MeV and twelve double planes - 0% B.C. DNN method, without false positives, Stochastic Shut-Off Scenario.

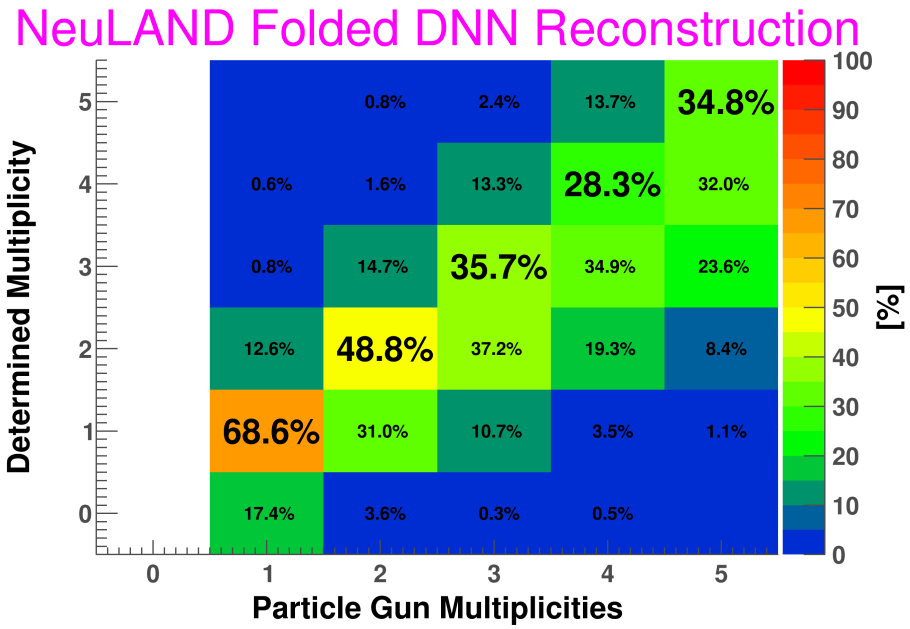

Figure 18: The obtained Multiplicity Prediction with two-neutron events and neutron energies of 1000 MeV and twelve double planes - 5% B.C. DNN method, Stochastic Shut-Off Scenario.

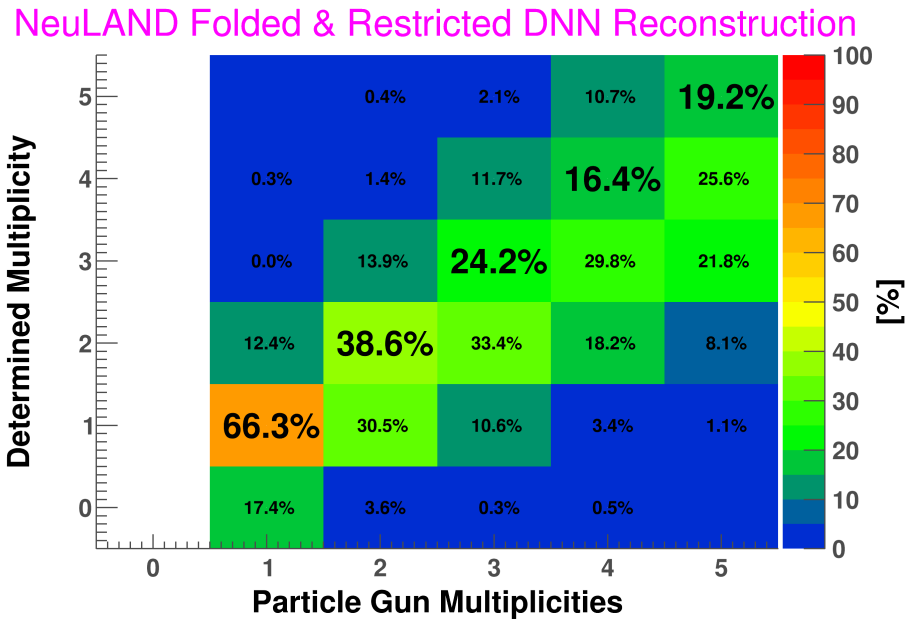

Figure 19: The obtained Multiplicity Prediction with two-neutron events and neutron energies of 1000 MeV and twelve double planes - 5% B.C. DNN method, without false positives, Stochastic Shut-Off Scenario.

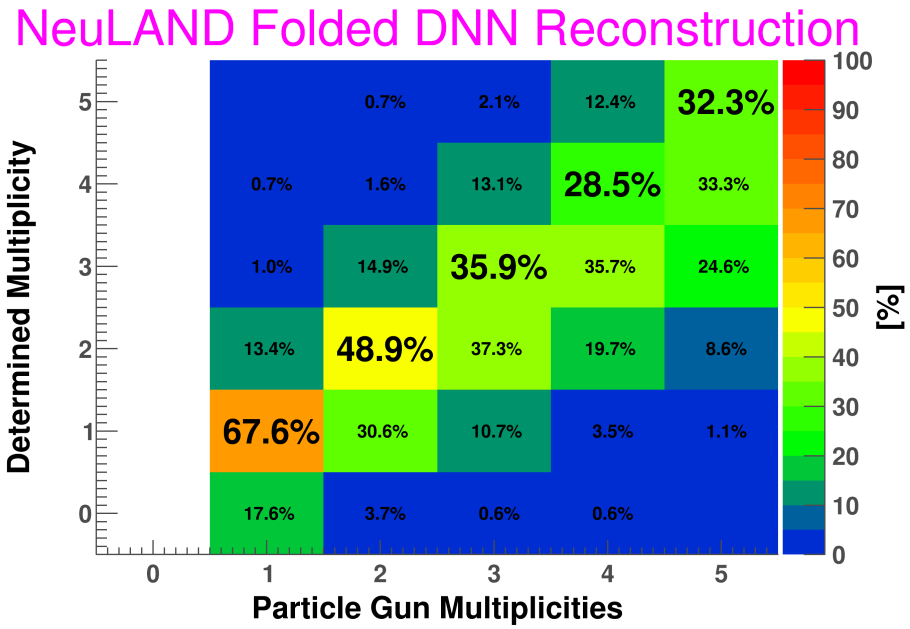

Figure 20: The obtained Multiplicity Prediction with two-neutron events and neutron energies of 1000 MeV and twelve double planes - 10% B.C. DNN method, Stochastic Shut-Off Scenario.

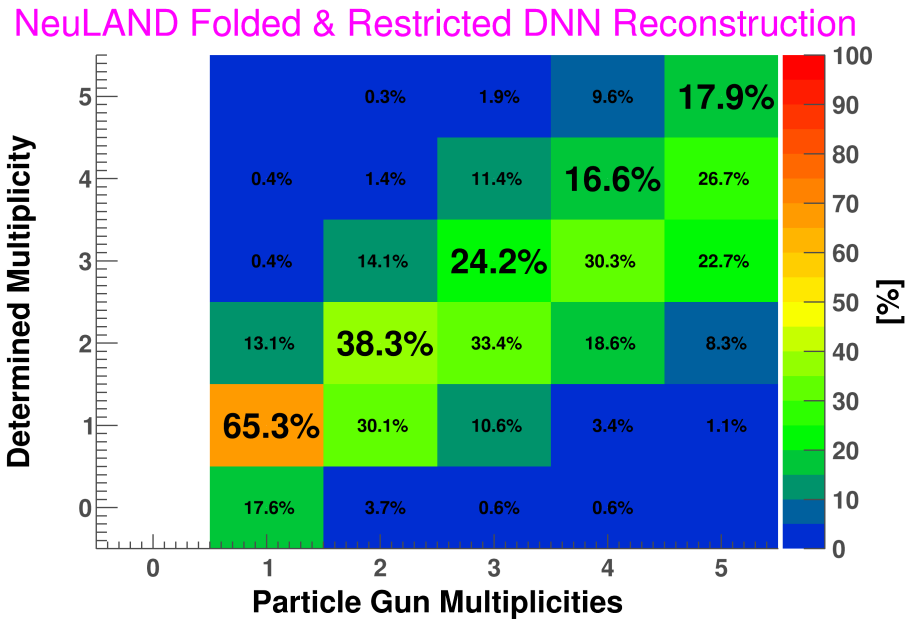

Figure 21: The obtained Multiplicity Prediction with two-neutron events and neutron energies of 1000 MeV and twelve double planes - 10% B.C. DNN method, without false positives, Stochastic Shut-Off Scenario.

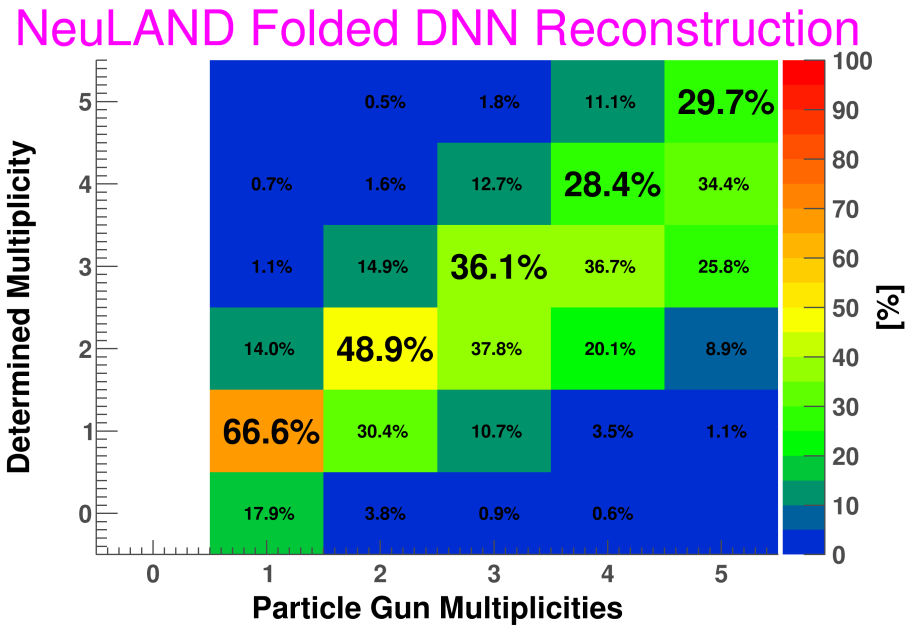

Figure 22: The obtained Multiplicity Prediction with two-neutron events and neutron energies of 1000 MeV and twelve double planes - 15% B.C. DNN method, Stochastic Shut-Off Scenario.

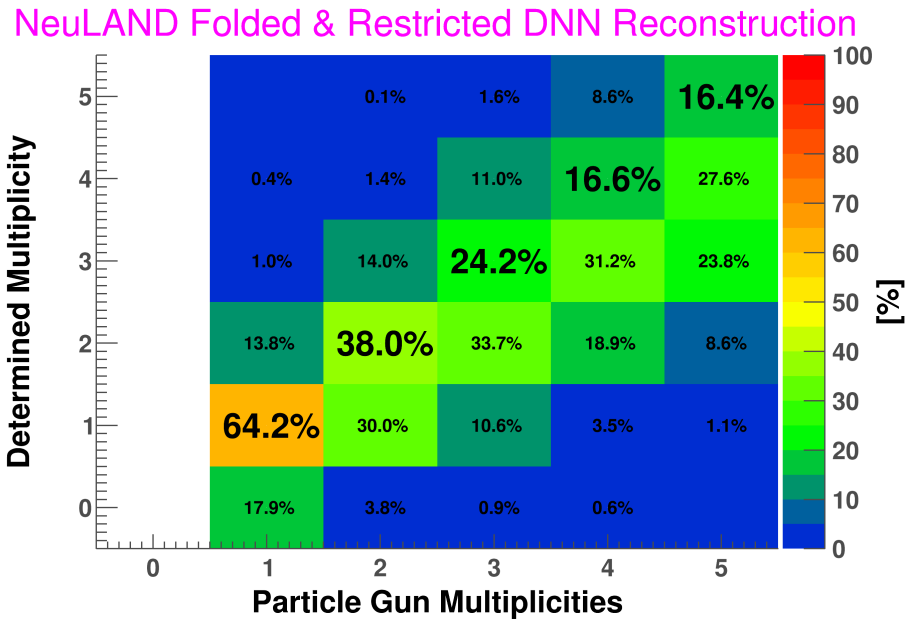

Figure 23: The obtained Multiplicity Prediction with two-neutron events and neutron energies of 1000 MeV and twelve double planes - 15% B.C. DNN method, without false positives, Stochastic Shut-Off Scenario.

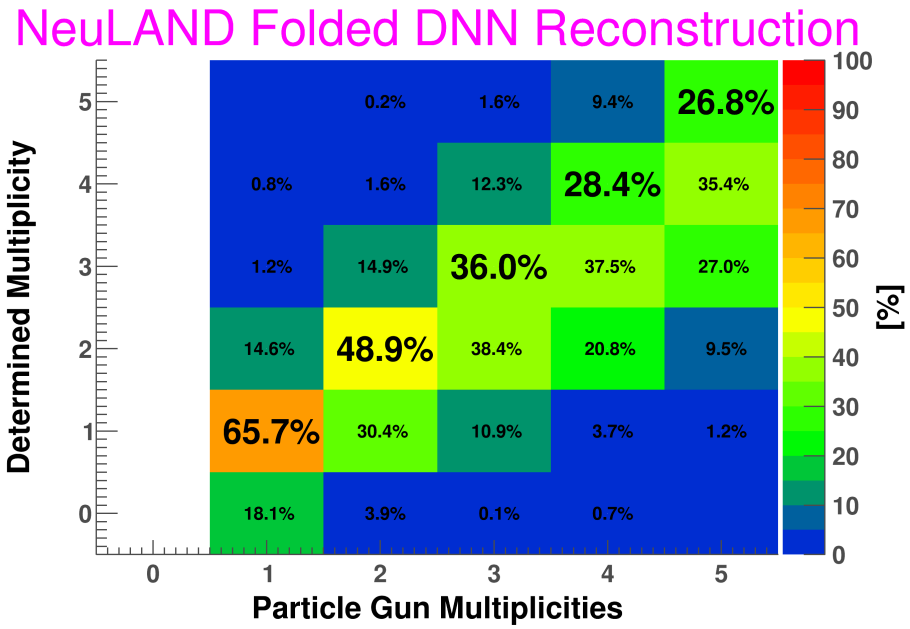

Figure 24: The obtained Multiplicity Prediction with two-neutron events and neutron energies of 1000 MeV and twelve double planes - 20% B.C. DNN method, Stochastic Shut-Off Scenario.

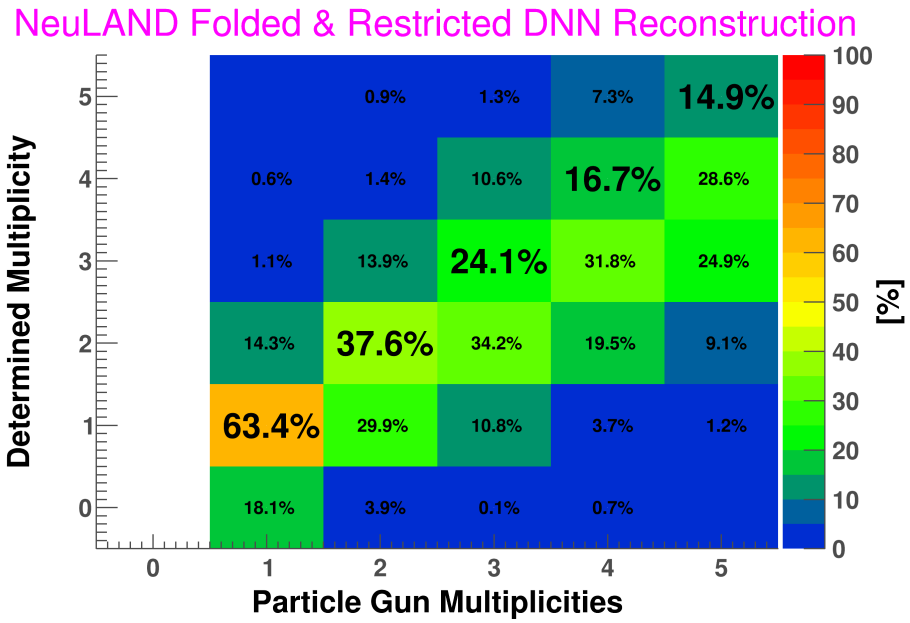

Figure 25: The obtained Multiplicity Prediction with two-neutron events and neutron energies of 1000 MeV and twelve double planes - 20% B.C. DNN method, without false positives, Stochastic Shut-Off Scenario.

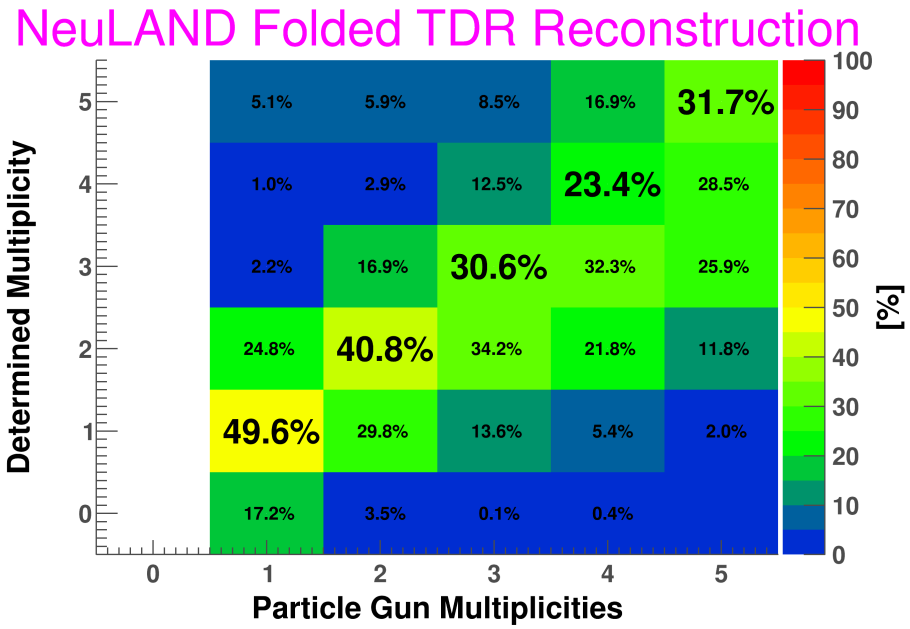

Figure 26: The obtained Multiplicity Prediction with two-neutron events and neutron energies of 1000 MeV and twelve double planes - 0% B.C. TDR method, Stochastic Shut-Off Scenario.

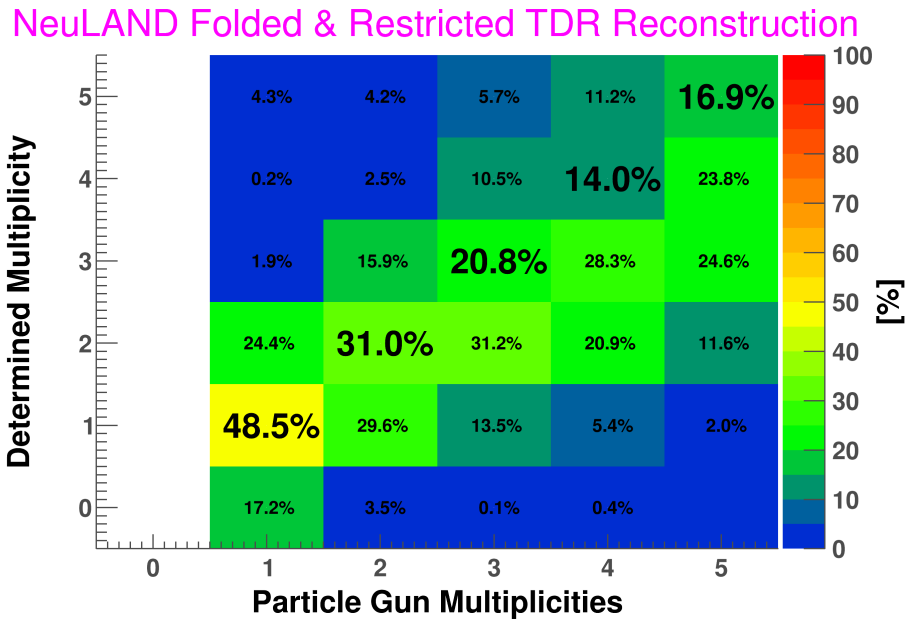

Figure 27: The obtained Multiplicity Prediction with two-neutron events and neutron energies of 1000 MeV and twelve double planes - 0% B.C. TDR method, without false positives, Stochastic Shut-Off Scenario.

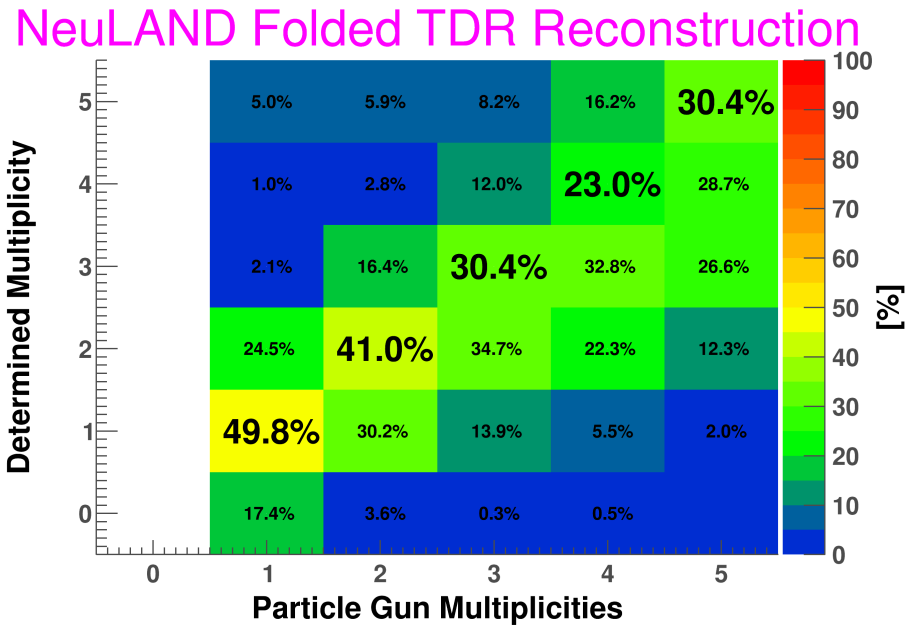

Figure 28: The obtained Multiplicity Prediction with two-neutron events and neutron energies of 1000 MeV and twelve double planes - 5% B.C. TDR method, Stochastic Shut-Off Scenario.

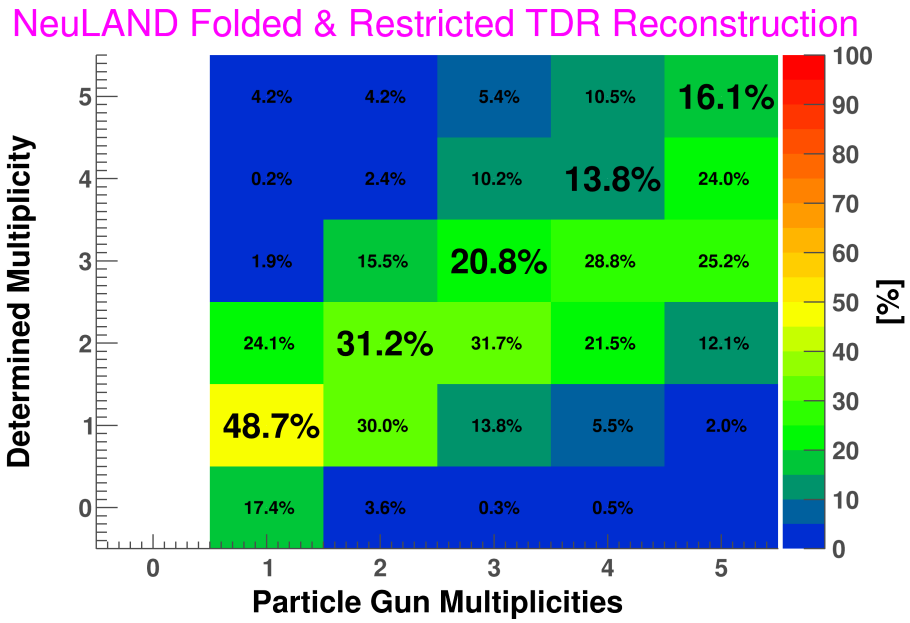

Figure 29: The obtained Multiplicity Prediction with two-neutron events and neutron energies of 1000 MeV and twelve double planes - 5% B.C. TDR method, without false positives, Stochastic Shut-Off Scenario.

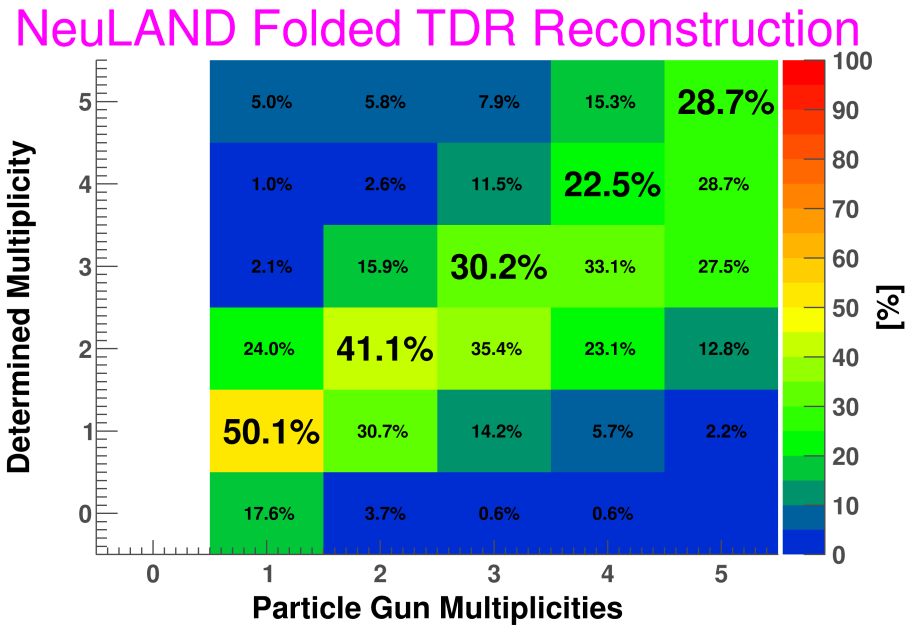

Figure 30: The obtained Multiplicity Prediction with two-neutron events and neutron energies of 1000 MeV and twelve double planes - 10% B.C. TDR method, Stochastic Shut-Off Scenario.

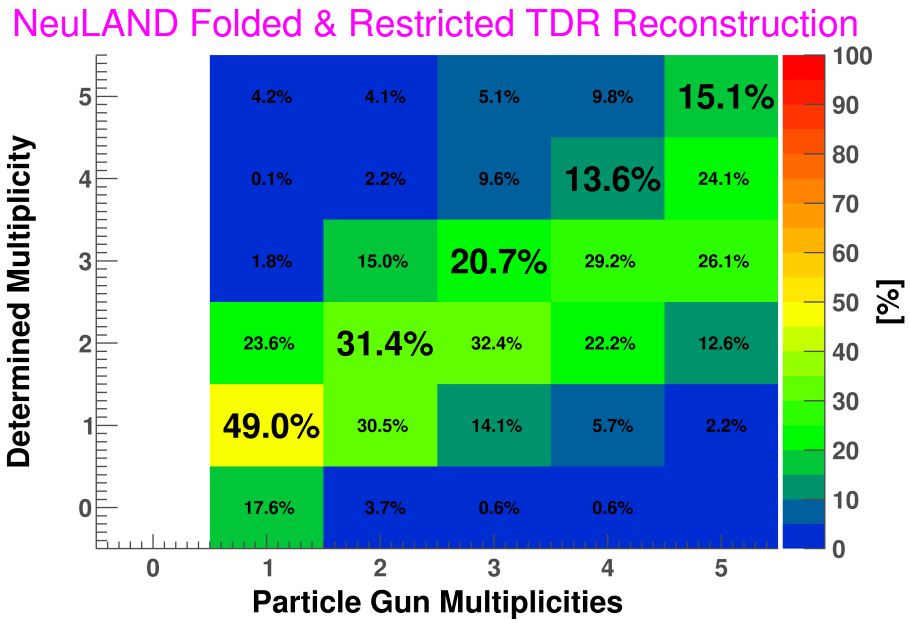

Figure 31: The obtained Multiplicity Prediction with two-neutron events and neutron energies of 1000 MeV and twelve double planes - 10% B.C. TDR method, without false positives, Stochastic Shut-Off Scenario.

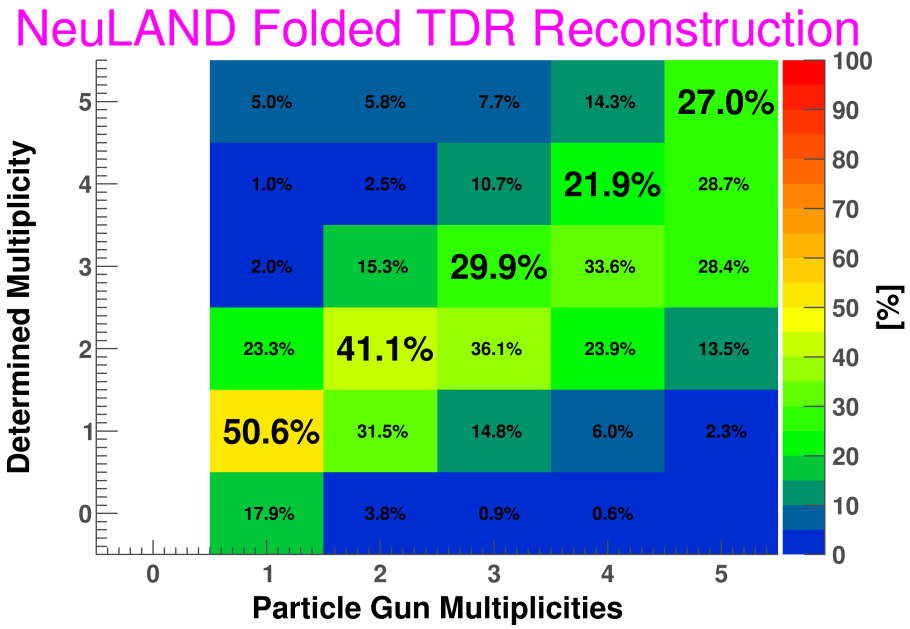

Figure 32: The obtained Multiplicity Prediction with two-neutron events and neutron energies of 1000 MeV and twelve double planes - 15% B.C. TDR method, Stochastic Shut-Off Scenario.

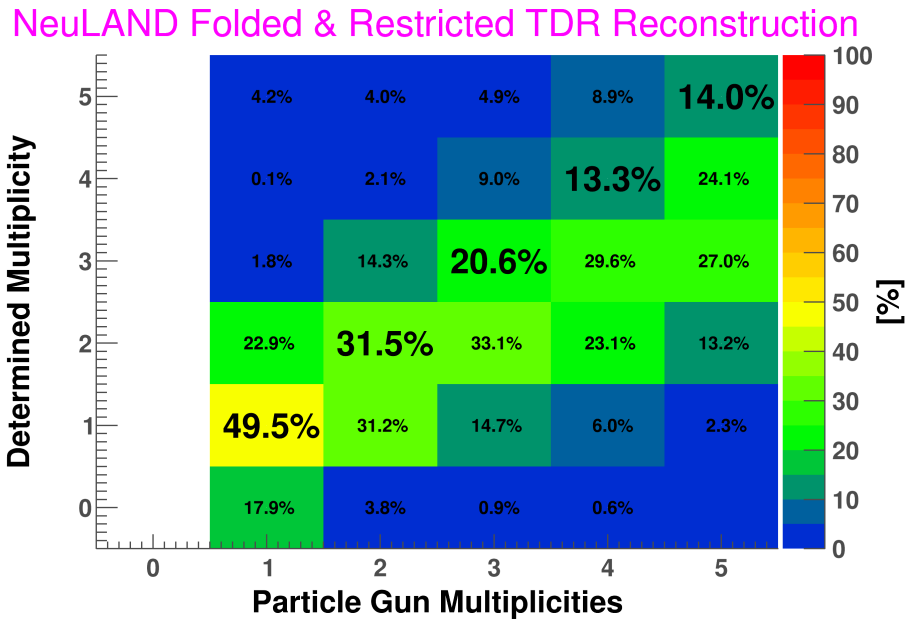

Figure 33: The obtained Multiplicity Prediction with two-neutron events and neutron energies of 1000 MeV and twelve double planes - 15% B.C. TDR method, without false positives, Stochastic Shut-Off Scenario.

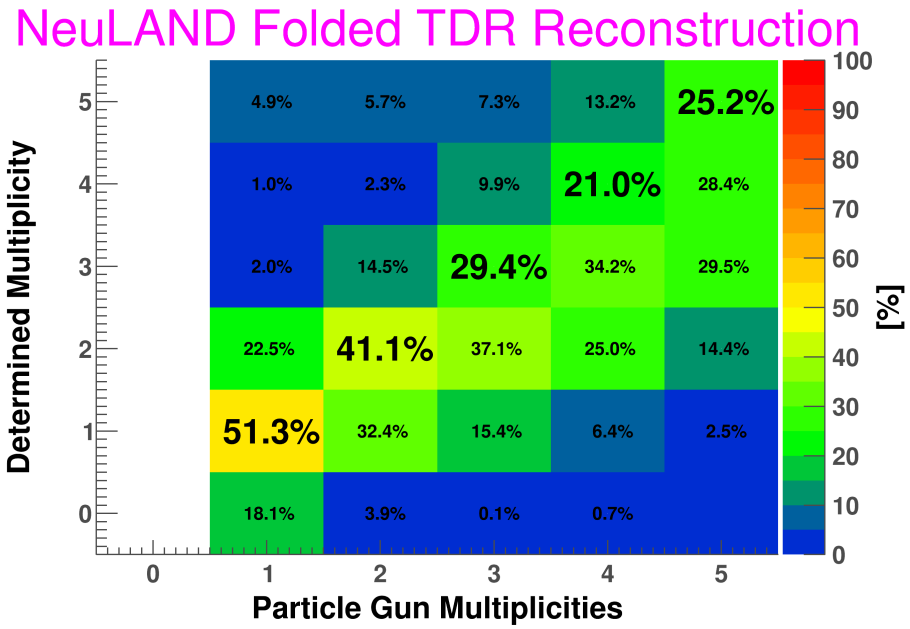

Figure 34: The obtained Multiplicity Prediction with two-neutron events and neutron energies of 1000 MeV and twelve double planes - 20% B.C. TDR method, Stochastic Shut-Off Scenario.

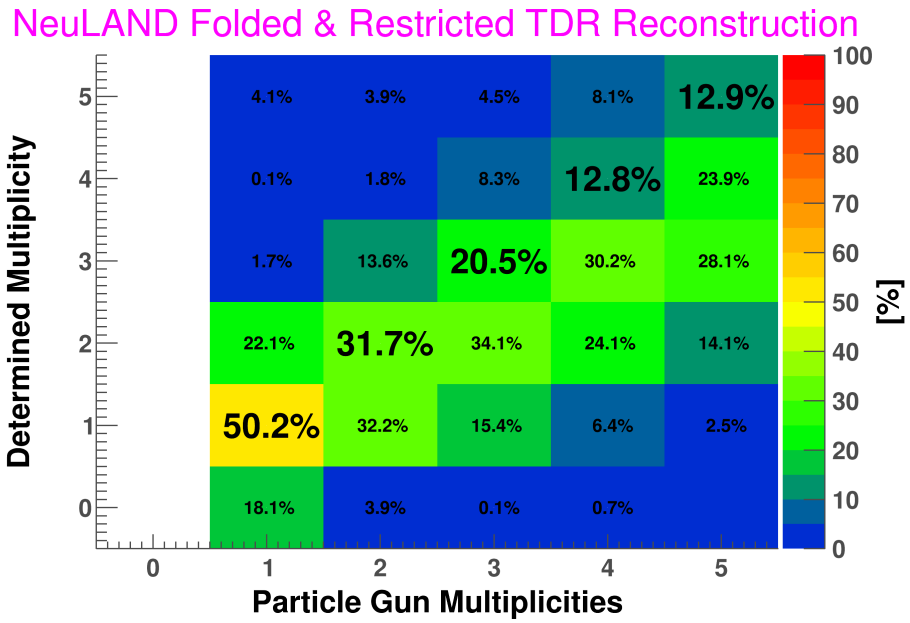

Figure 35: The obtained Multiplicity Prediction with two-neutron events and neutron energies of 1000 MeV and twelve double planes - 20% B.C. TDR method, without false positives, Stochastic Shut-Off Scenario.

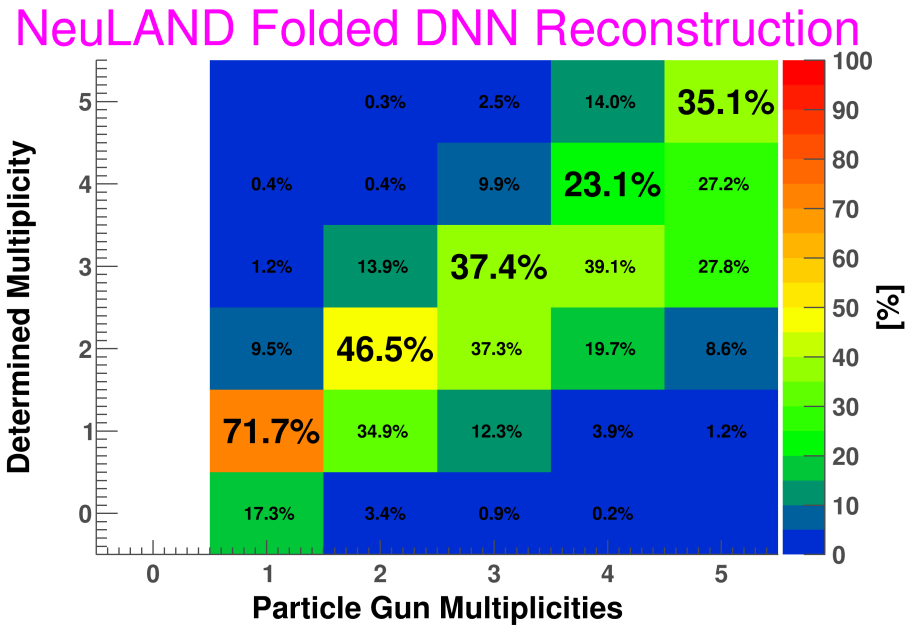

Figure 36: The obtained Multiplicity Prediction with two-neutron events and neutron energies of 1000 MeV and twelve double planes - 0 B.M. DNN method, Worst-Case Scenario.

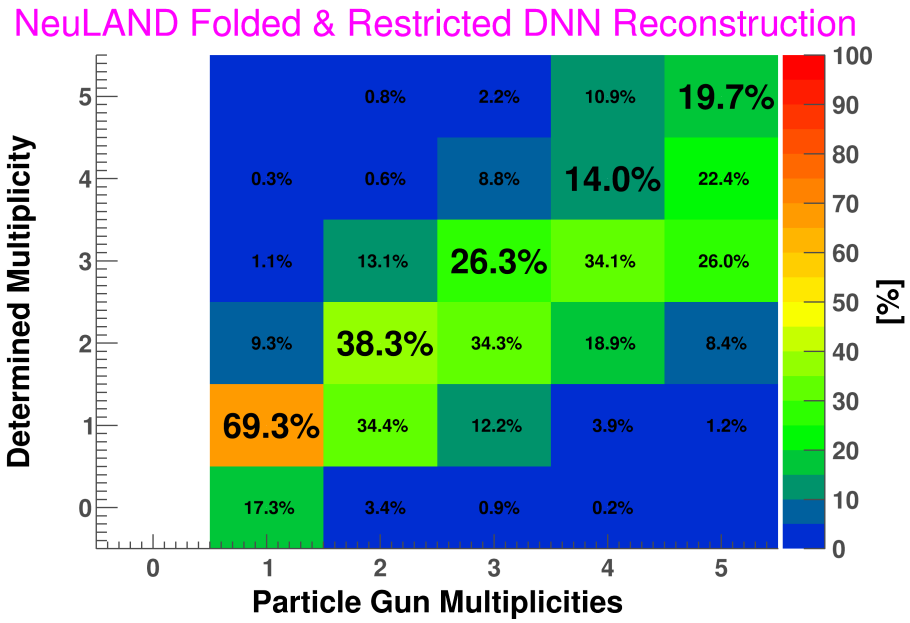

Figure 37: The obtained Multiplicity Prediction with two-neutron events and neutron energies of 1000 MeV and twelve double planes - 0 B.M. DNN method, without false positives, Worst-Case Scenario.

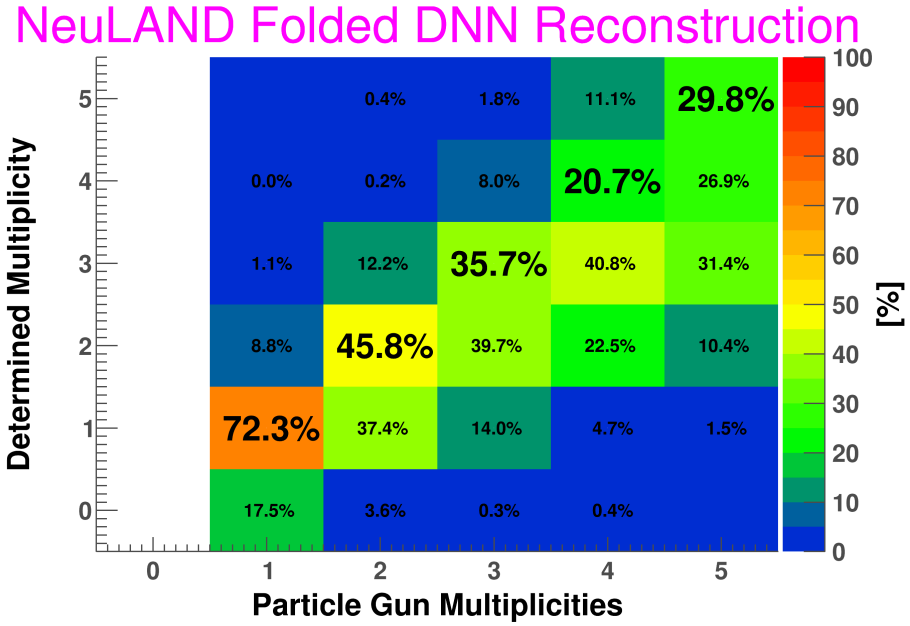

Figure 38: The obtained Multiplicity Prediction with two-neutron events and neutron energies of 1000 MeV and twelve double planes - 2 B.M. DNN method, Worst-Case Scenario.

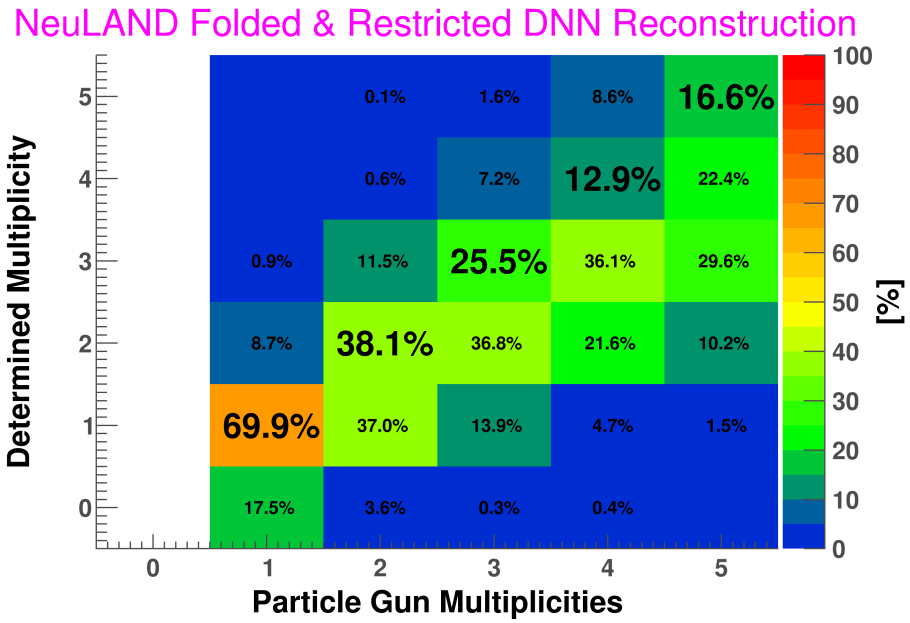

Figure 39: The obtained Multiplicity Prediction with two-neutron events and neutron energies of 1000 MeV and twelve double planes - 2 B.M. DNN method, without false positives, Worst-Case Scenario.

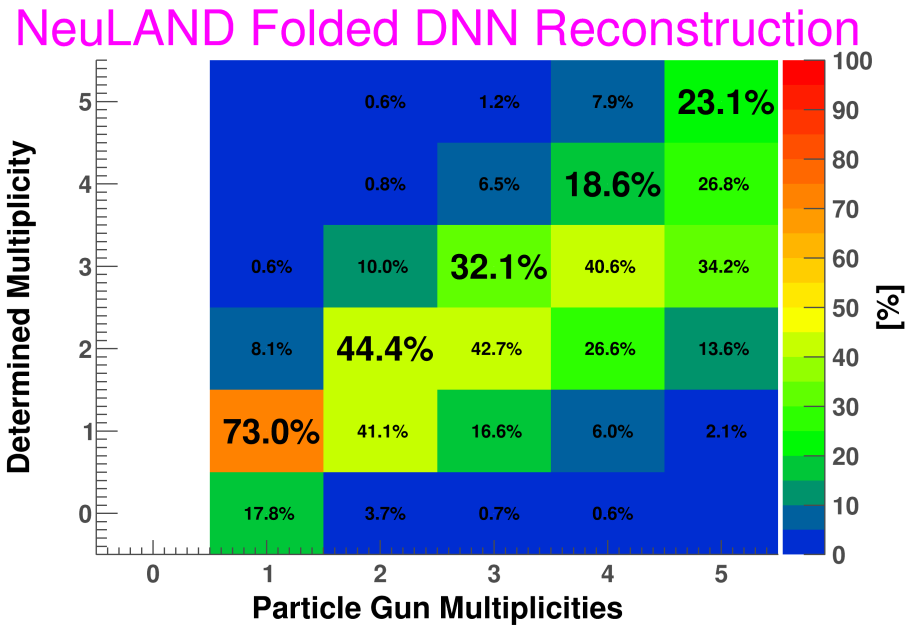

Figure 40: The obtained Multiplicity Prediction with two-neutron events and neutron energies of 1000 MeV and twelve double planes - 4 B.M. DNN method, Worst-Case Scenario.

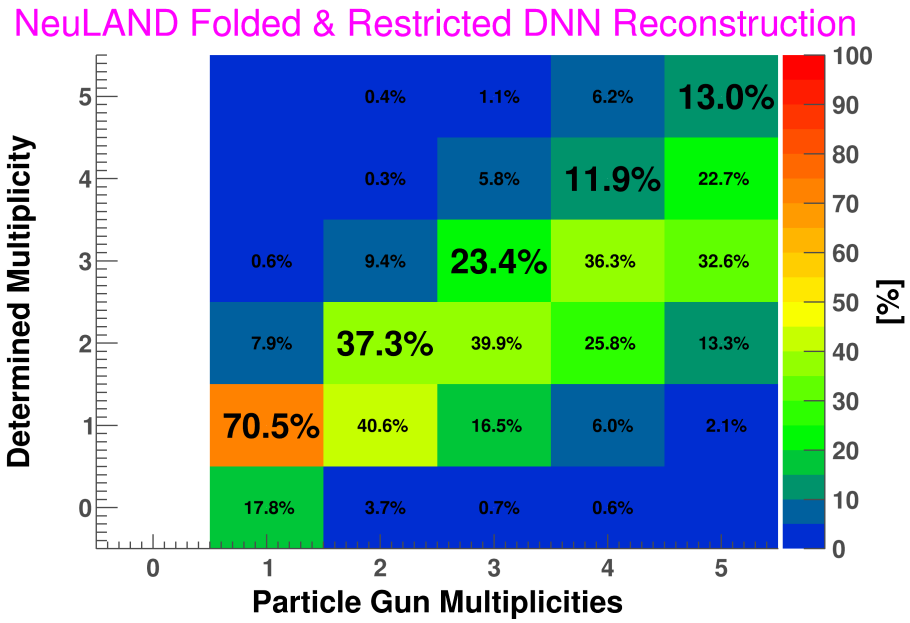

Figure 41: The obtained Multiplicity Prediction with two-neutron events and neutron energies of 1000 MeV and twelve double planes - 4 B.M. DNN method, without false positives, Worst-Case Scenario.

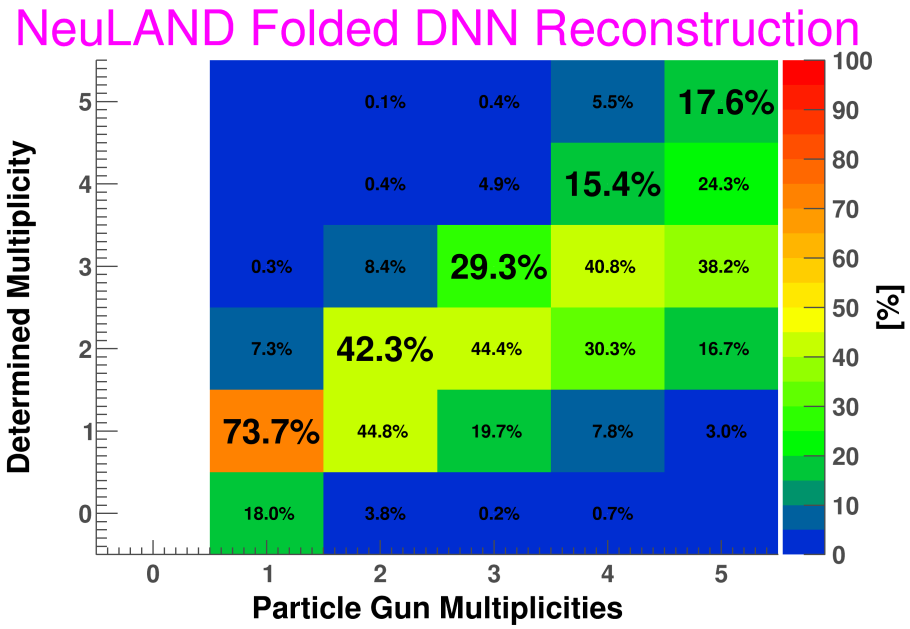

Figure 42: The obtained Multiplicity Prediction with two-neutron events and neutron energies of 1000 MeV and twelve double planes - 6 B.M. DNN method, Worst-Case Scenario.

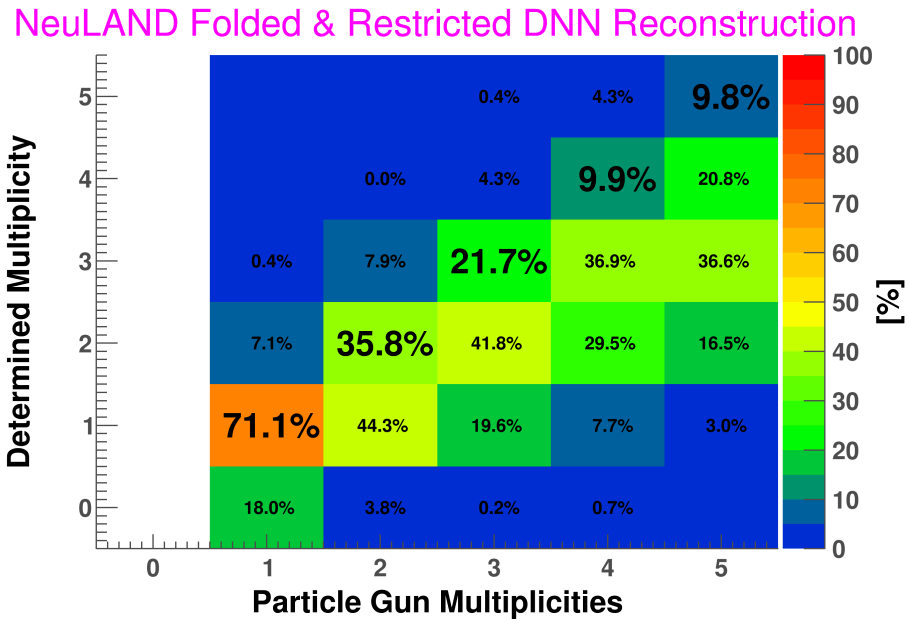

Figure 43: The obtained Multiplicity Prediction with two-neutron events and neutron energies of 1000 MeV and twelve double planes - 6 B.M. DNN method, without false positives, Worst-Case Scenario.

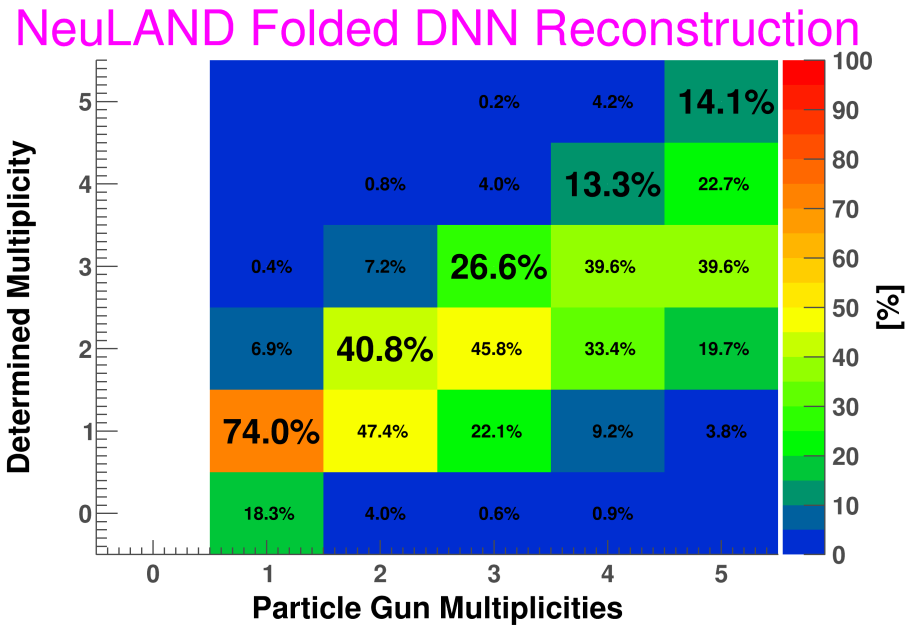

Figure 44: The obtained Multiplicity Prediction with two-neutron events and neutron energies of 1000 MeV and twelve double planes - 8 B.M. DNN method, Worst-Case Scenario.

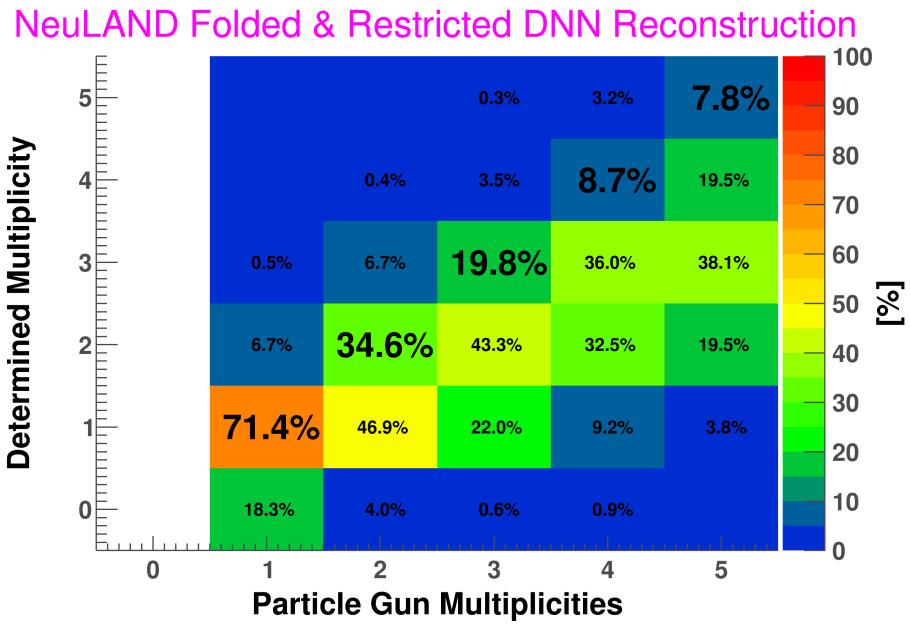

Figure 45: The obtained Multiplicity Prediction with two-neutron events and neutron energies of 1000 MeV and twelve double planes - 8 B.M. DNN method, without false positives, Worst-Case Scenario.